Report No. BC354 RPWO #47 – Part 2 December 2002
FINAL REPORT

Contract Title: Evaluation of Precast Box Culvert Systems
UF Project No. 4910 4504 857 12
Contract No. BC354 RPWO #47 – Part 2

DESIGN LIVE LOADS ON BOX CULVERTS

Principal Investigators: Ronald A. Cook
David Bloomquist

Graduate Research Assistant: A.J. Gutz

Project Manager: Marcus H. Ansley

Department of Civil & Coastal Engineering
College of Engineering
University of Florida
Gainesville, Florida 32611

Engineering and Industrial Experiment Station

Technical Report Documentation Page

1. Report No. BC354 RPWO #47 – Part 2	2. Government Accession No.	3. Recipient's Catalog No.
4. Title and Subtitle Evaluation of Precast Box Culvert Systems Design Live Loads on Box Culverts		5. Report Date December 2002 6. Performing Organization Code
7. Author(s) D. G. Bloomquist and A.J. Gutz		8. Performing Organization Report No. 4910 4504 857 12
9. Performing Organization Name and Address University of Florida Department of Civil Engineering 345 Weil Hall / P.O. Box 116580 Gainesville, FL 32611-6580		10. Work Unit No. (TRAIS) 11. Contract or Grant No. BC354 RPWO #47 – Part 2
12. Sponsoring Agency Name and Address Florida Department of Transportation Research Management Center 605 Suwannee Street, MS 30 Tallahassee, FL 32301-8064		13. Type of Report and Period Covered Final Report 14. Sponsoring Agency Code

15. Supplementary Notes

Prepared in cooperation with the Federal Highway Administration

16. Abstract

This report discusses the development of equations to calculate live loads for the design of precast concrete box culverts. The equations generate a uniformly distributed live load based on the depth of fill above the culvert. The method of superposition was used to calculate stresses on the box culvert's top slab. The American Association of State Highway and Transportation Officials (AASHTO) design tandem and design truck loads were used in the generation of the expected live loads. These loads were then used to calculate shears and moments in the culverts slab. An equivalent uniform load that produced the same maximum shear or moment as did the AASHTO trucks was then computed. These equivalent loads were then plotted versus soil depth to develop design equations. Based on the results, the final design equation may eventually be used in lieu of the AASHTO method currently used to generate design live loads. The calculated stresses, as well as the shears and moments, match closely to those generated by the AASHTO method. The final equation should offer the design engineer a significant saving of both time and energy, without sacrificing accuracy or effectiveness. This final design equation could possibly be verified and refined by field testing; namely a field loading of a culvert. Recommendations for further study are included.

17. Key Words Precast Box Culverts, Box Culverts, Arch Culverts	18. Distribution Statement No restrictions. This document is available to the public through the National Technical Information Service, Springfield, VA, 22161

19. Security Classif. (of this report)	20. Security Classif. (of this page)	21. No. of Pages	22. Price
Unclassified	Unclassified	88	

Form DOT F 1700.7 (8-72)

EVALUATION OF PRECAST BOX CULVERT SYSTEMS
DESIGN LIVE LOADS ON BOX CULVERTS

Contract No. BC 354 RPWO #47 – Part 2
UF No. 4910 4504 857 12

Principal Investigators:	Ronald A. Cook David Bloomquist
Graduate Research Assistant:	A.J. Gutz
FDOT Technical Coordinator:	Marcus H. Ansley

Engineering and Industrial Experiment Station
Department of Civil Engineering
University of Florida
Gainesville, Florida

December 2002

TABLE OF CONTENTS

LIST OF TABLES

LIST OF FIGURES

CHAPTER 1
INTRODUCTION

A roadway sometimes must span a small ditch, irrigation canal or other small body of water. Often, a bridge is too large and costly a solution to protect the roads right of way. When this is true, a box culvert is an ideal solution. Box culverts are constructed of reinforced concrete and are either cast-in-place or precast. There is a current trend to use more precast box culvert systems for their ease of installation and better ability to monitor quality control. Box culverts are in effect large buried pipes. They control water flow and drainage for irrigation and municipal services, control storm water, and perform many other services. They vary in size from a cross section of 3 ft by 3 ft to 12 ft by 12 ft and larger. They are not all square dimensions; but if not a square, usually have the span length exceeding the opening height. Box culverts may have multiple or single cell openings.

1.1 Purpose

In situations where the box culvert is under a roadway, it is considered a bridge and designed as such. The American Association of State Highway and Transportation Officials (AASHTO) LRFD design code was applied as the design standard for all structures in the Florida Department of Transportation (FDOT) system starting in 1998. Such a rigorous design method is thought to be extremely difficult to apply and too conservative when compared to the previous code. The major concern was with the live load mechanism used to determine the most critical load on the culvert. The purpose of this project was to determine a new method for generating design live loads for concrete box culverts. By simplifying this portion of the design process, a significant saving of design time could be achieved. Also, this work was aimed at producing a design that would be sound but not overly conservative.

1.2 Scope

The approach of the research that was conducted for this thesis is as follows:

- Theoretical methods were used to calculate the loads on a culvert for different depths of fill above the culvert. Results were compared to the loads generated using the AASHTO method.
- The shears and moments in culverts of different spans were found based on the loading from the AASHTO trucks found in the above step.
- Knowing the maximum shears and moments from the above step, an equivalent uniform load model was developed, based on statics, which produced the same peak moment at different depths of fill.

Chapter 2 describes methods of stress calculation, as well as relevant field work. Chapter 3 explains how load distributions were used to generate shears and moments in the slab of the culvert and how they were used to generate an equivalent uniformly distributed live load. Chapter 4 presents equations that were developed that predict the equivalent uniformly distributed live loads based on the depth of fill. Chapter 5 explains the final design equation and gives recommendations for future work.

CHAPTER 2
LITERATURE REVIEW

This section compares the current AASHTO LRFD design methodology, to the old Standard Design specification, as well as traditional methods used to calculate loads under fill. It also describes field tests where box culverts were subject to live load conditions.

2.1 Design Methodology

In 1994, AASHTO introduced the load and resistance factor design (LRFD) Bridge Design Specification methodology. Its goal was to provide a reliability-based code that offered a more uniform level of safety than the existing Standard Specification for Highway Bridges [1]. Both specifications used load factors and strength reduction factors, however the LRFD attempts to account for variability in loading and the resistance of structural elements. To achieve this, there are a number of changes from the Standard Specification to the LRFD Specification. Many of these changes relate to the mechanism used to produce the most critical combination of live load on the box culvert. Some of these changes include the load factors and modifiers, multiple presence factors, design vehicle loads, distribution of live load through fill, and the dynamic load allowance. There are other differences in the specifications, however the above are among the most important as far as live load is concerned.

Load factors reflect a measure of uncertainty in the accuracy of a specific type of load, or combination of loads. Load modifiers are related to ductility, redundancy, and importance. Based on these three criteria, load factors can be increased or decreased. The Standard Specification used the concept of load factors, but not load modifiers. The value of the live load factor for the Standard Specification is 2.17, and for the LRFD Specification, the live load factor is 1.75. This is the largest change in all the load factors from the Standard to the LRFD Specification.

This large change in the value of the live load factor is accounted for with the multiple presence factors. Its value is dependant upon the number or loaded lanes. According to the LRFD Specification, the multiple presence factor is 1.2 for a single loaded lane, 1.0 for two loaded lanes, 0.85 for 3 loaded lanes and 0.65 for 4 or more loaded lanes [2]. The multiple presence factor is similar to the load reduction factor in the Standard Specification. By comparison, the Standard gives a value of 1.0 for one or two loaded lanes, 0.90 for three loaded lanes and 0.75 for four or more loaded lanes [3]. The increase from 1.0 to 1.2 for one loaded lane balances the reduction in the load factor described above.

Another change from the Standard to the LRFD Specification has to do with the vehicle design loads. The LRFD requires two types of design vehicles: the design truck and the design tandem. The design truck is the same as the HS20 truck in the Standard Specification. However, the load for the design tandem was increased from a 24 kip axle load to a 25 kip axle load. Also, the LRFD specification requires that both the design truck and design tandem must be accompanied by the design lane load. The design lane load is equal to 640 lb/ft distributed uniformly over a 10 foot wide lane.

Distribution of the live load through fill is another provision that changed from the Standard to the LRFD code. For fill depths less than 2 ft, both codes use the equivalent strip method, however with some differences in each method. There are also changes for depths of fill of 2 ft and greater. These changes are more applicable for this project. According to the LRFD code, for a depth of fill of 2 ft and greater, the wheel loads act over the tire footprint. The footprint's dimensions are increased by 1.15 for select granular backfill, or by 1.0 for all other types of fill (Figure 2-1). By comparison, the Standard code treats the wheel loads as a point load and distributes them over an area equal to a square with dimensions of 1.75 times the depth of fill (Figure 2-2). The LRFD method often yields greater design forces than the Standard, especially for shallow cover [1].

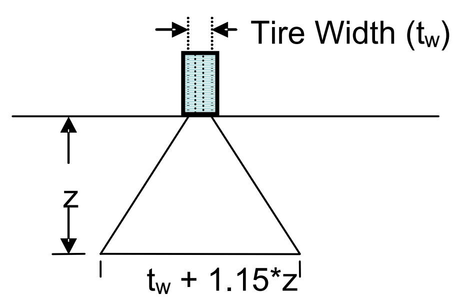

Figure 2-1. The AASHTO LRFD live load distribution

The dynamic load allowance accounts for the impact of moving vehicles. In the LRFD, its value varies linearly from a 33% increase at 0 ft of fill to 0% increase at 8 ft of fill. For the Standard Specifications it takes the form of a multiplier. The dynamic load allowance multiplier is 1.3 at 0 ft of fill and decreases in 10% steps to 1.0 at 3 ft of fill and greater. This dynamic load allowance is also called the impact factor. The dynamic load allowance and the load factor also act to increase the tire contact area according to the LRFD code. The Standard Specification does not account for an increase in the tire contact area from the impact load factor. This increase in the tire contact is significant considering how it is used to distribute the load through fill as discussed above.

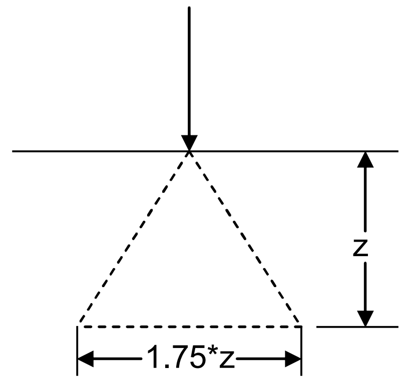

Figure 2-2. The AASHTO standard specification load distribution

2.2 Methods for Calculating Loads under Fill

2.2.1 Point Loads

Many of the current methods to calculate the stress in a soil mass from an external load are based on elastic theory. The application of this theory includes the assumptions that the soil is homogeneous and isotropic. Soil usually seriously violates this assumption, however the methods based on elastic theory have proven effective so long as they are combined with sound engineering judgment. Also, there is the assumption that the stress is proportional to the strain. So long as the stress increase is well below failure the strains should be approximately proportional to the stresses [4]. It should be noted that for all the methods outlined below, the stress calculated is the increase in stress due to the live load at the surface; the geostatic stresses are not included in these calculations.

One method to determine the state of stress within an elastic, homogeneous and isotropic half-space was developed by Boussinesq in 1855 [4]. His method considered the stress increase based on a point load acting perpendicular to the surface. The value of the vertical stress may be calculated as

$$\sigma_z = \frac{P\left(3z^3\right)}{2\pi\left(r^2 + z^2\right)^{5/2}} \tag{1-1}$$

where P = point load

z = depth from ground surface to where σ_z is desired

r = horizontal distance from point load to where σ_z is desired

This is shown below in Figure 2-1.

Figure 2-3. Boussinesq point load

Soil deposits found naturally do not approach the ideal conditions that the above equation is based upon. Many soil deposits were made by the sedimentation of alternating clay and silt layers. These soils are called varved clays. Westergaard in 1938 proposed a solution that was applicable for these type of deposits [4]. In his theory, an elastic soil is interspersed with infinitely thin but perfectly rigid layers that only allow for vertical displacement, but no horizontal displacement [4]. Using his theory, the vertical stress may be calculated as

$$\sigma_z = \frac{P}{z^2\pi} * \frac{1}{\left[1+2\left(\frac{r}{z}\right)^2\right]^{3/2}} \qquad (1\text{-}2)$$

where the variables are the same as defined above. Both methods produce approximately the same results, therefore it is a matter of preference as to which on should be used. However, if it were known that the soil at the point in question was indeed layered as Westergaard assumed, his method may be slightly more accurate.

2.2.2 Superposition

In some situations, the actual loading is not acting at a point, but over some area, such as is the case for the wheel loads in the LRFD specification. In this type of situation, it is advantageous to have a method of calculating stress at a depth based on a patch load. To achieve this, the above Boussinesq solution was integrated over a to line get an equation based on a line load. Newmark integrated the equation based on a line load in 1935 and it gave an equation for the stress under the corner of a uniformly loaded rectangular area [4].

$$\sigma_z = q_o * \frac{1}{4\pi}\left[\frac{2mn\left(m^2+n^2+1\right)^{1/2}}{m^2+n^2+1+m^2n^2} * \frac{m^2+n^2+2}{m^2+n^2+1} + \arctan\frac{2mn\left(m^2+n^2+1\right)^{1/2}}{m^2+n^2+1-m^2n^2}\right] \qquad (1\text{-}3)$$

where q_o = the contact stress at the surface

m = x/z

n = y/z

x, y = length and width of the uniformly loaded area

z = depth from surface to point where stress increase is desired

For simplicity, the portion of the above equation in brackets is known as *I*, or the influence value. This method can also be used for locations that are outside of the loaded area. Rectangles can be constructed that each have corners above the point in question, and are added or subtracted as necessary.

2.2.3 Buried Pipe Method

Another situation that calls for the calculation of increases in stress at depth due to surface live loads is in the design of buried pipe. Although the geometry of a box culvert is different to that of a pipe, they serve approximately the same purpose, and are often subjected to the same conditions. Therefore this method of calculating stresses on buried pipes was applied to box culverts as well.

The method described here is another based on the original Boussinesq solution, therefore all the inherent limitations that the Boussinesq solution had are present. The Boussinesq solution was integrated to produce a load coefficient to be used in an equation that would predict the load on a pipe in units of force per length [5]. This load coefficient is based on the pipes dimensions and geometry. The equation is shown below:

$$W_{sd} = C_s p F' B_c \tag{1-4}$$

where W_{sd} = load on pipe in lb/unit length

p = intensity of distributed load in psf

F' = impact factor

B_c = diameter of pipe in feet

C_s = load coefficient which is a function of D/(2H) and M/(2H), where D and M are the width and length, respectively, of the area over which the distributed load acts [5].

This equation considers the load at the surface to be a distributed load. There is another solution for when the surface load is a point load, however for this study the assumption that the surface load is a distributed appears to be more valid than assuming that it is a point load. Values for the impact factor, F', and the load coefficient, C_s, were given in tables in the text [5].

2.2.4 The AASHTO, 2:1, and ASCE Methods

One of the simplest methods to calculate the distribution of load with depth is known as the 2:1 method. The AASHTO LRFD method is a variation of this method. The ASCE standard follows similar guidelines as those in the AASHTO specification. The 2:1 method is an empirical approach that assumes that the area over which the load acts increases in a systematic way with depth [4]. An increase in area corresponds to a decrease in stress for a given surface load. At a given depth z, the enlarged area increases by z/2 on each side. Therefore the live load stress can be calculated as

$$\sigma_z = \frac{load}{(B+z)(L+z)} \qquad (1\text{-}5)$$

where σ_z = live load stress. B, L = width and length, respectively, of the loaded area at the surface. This is a somewhat crude method, but is often used for its simplicity.

The AASHTO LRFD method is a variation of this method. The AASHTO LRFD specification states that wheel loads may be considered to be uniformly distributed over a rectangular area with sides equal to the dimension of the tire contact area and increased by 1.15 times the depth of fill for select granular fill, and increased by the depth of fill for all other types of fill (Figure 2-1).

The AASHTO LRFD specification also states that where such areas from multiple wheels overlap, the total load shall be uniformly distributed over the area. This is shown in Figure 2-4. It is the opinion of the FDOT that this provision can lead to very conservative stresses being used for design. The ASCE specification is another variation;

it is the same as the AASHTO, however it states that the loaded area is increased by 1.75 times the depth of fill for all types of fill [6]. The ASCE specifications also differ in that the live load should not be arbitrarily eliminated at a depth of fill of 8 ft, as in the AASHTO specifications [6].

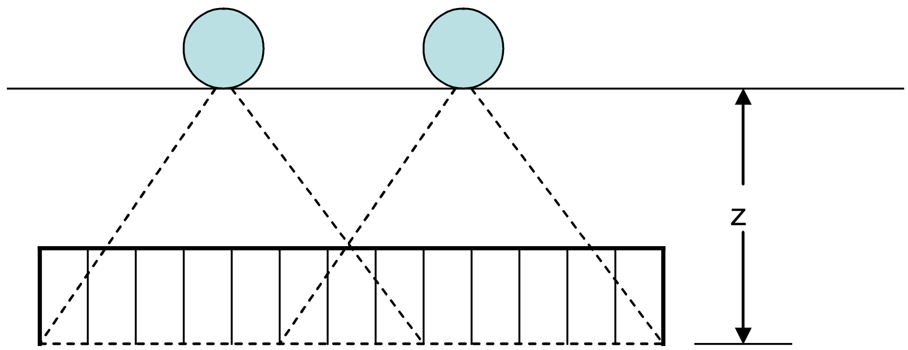

Figure 2-4. AASHTO overlapping load distribution

2.3 Field Loading of Culverts

This section describes two field loading tests of full size reinforced concrete box culverts. One test was completed by Texas A & M University and the University of Nebraska completed the other. Both of these tests involved rigging a full size culvert with load cells and placing various amounts of fill above the culvert. Loaded trucks were then driven over the culvert and stresses at the top culvert slab were measured.

2.3.1 Texas A & M

An eight foot by eight foot by forty-four foot long reinforced concrete box culvert was constructed and instrumented with pressures cells in 1982. Tests were completed from 1982 to 1984. Twelve pressure cells were installed flush with the top slab of the culvert. Live loads were applied by parking a test vehicle at designated locations above the culvert and recording the static earth pressure [7]. The pressure recorded with no live load was subtracted from the test reading to measure the live load effects only. The truck used consisted of a five axle tractor-trailer with a rear tandem axle of two 24 kip axles spaced 4 ft apart. The other axles, a lightly loaded front tandem and the steering axle, were observed to have an insignificant effect compared to the heavily loaded rear tandem [7]. Depths of fill from 1 to 8 ft were placed above the culvert. It was attempted to develop an empirical equation that would fit the measured data.

Measured live load earth pressures were recorded at depths of 1, 2, 4, 6 and 8 ft of fill. For these depths, peak earth pressures were found to be 13.2 psi, 4.1 psi, 1.9 psi and 1.9 psi respectively. Boussinesq and Westergaard's equations along with other empirical equations were among the ones that were used to compare to the data. However, each of the equations were modified by certain best-fit parameters. Nonlinear regression was used to determine the values of these parameters. It was found that when the depth of fill was 4 ft or greater, the Boussinesq and Westergaard equations that were modified using nonlinear regression satisfactorily modeled the measured live load earth pressure [7]. For depths of fill equal to 2 ft or less, an empirically determined equation was found to best fit the measured data.

2.3.2 University of Nebraska

A similar test was completed by the University of Nebraska and described in a report from 1990. A two cell reinforced concrete box culvert was constructed and instrumented with load cells outside of Omaha, Nebraska. Each cell was 12 foot by 12 foot. Eight stations were set up above the culvert for the live load tests. Both wheel load tests and concentrated load tests were performed at these stations. For the wheel load tests, the rear axle was centered above each station; the concentrated load tests were performed by using a hydraulic jack to transfer the entire axle load through a single one square foot bearing plate [8]. The test truck consisted of a rear 22.8 kip double axle and a

4.2 kip front axle 14.1 ft apart. Tests were preformed in increments of 2 ft of fill. Pressures from the soil load only were subtracted from reading with the live load in place, therefore the presented loads were the net pressures due to the live load only.

A few observations were made based on the data gathered from the tests. First, at low fill heights, the pressure distribution was marked by isolated peaks at the point of application, with outside area exhibiting a near uniform distribution. This demonstrates little interaction between pressures caused by wheels on axles other than the tandem axle [8]. Second, at increasing depth, peaks decreased and the wheel loads were spread out over an increased area. Higher pressures were found in regions where those areas overlapped [8]. Also, the location of the maximum pressure moved from under the tandem's wheels to under the center of the tandem's axle at a depth of 8 ft. Another observation was that there was little interaction between the front and the rear axle. Only at depths of 10 ft and greater was any interaction noticed. Due to its distance from the heavily loaded rear axle and its much smaller load, it was suggested that the effect of the front driving axle could be neglected. This is the same conclusion that the previous Texas A & M study had found. Finally, it was found that load dispersion was nearly identical in both the longitudinal and transverse directions.

The report compared the measured field data to pressures predicted by the AASHTO method, using the 1.75 distribution factor. It was suggested that the 1.75 load factor could be used for all depths of fill, however, a nearly uniform pressure distribution was found at a depth of 8 ft of fill. This was due to the fact that the depth of fill also influenced the interaction between the wheel loads of the tandem. However, the effect of the live load diminished considerably at depths of 8 ft and greater [8]. Therefore, a suggested cut off for neglecting the live load effect is when it contributes less than five percent of the total load effects. Also, the report noted that the measured pressures contained higher peaks, however the AASHTO pressures still conservatively corresponded to a larger total load [8].

CHAPTER 3
CALCULATIONS AND RESULTS

This chapter summarizes the methods used to calculate the live load pressure for the 4 load conditions at various depths. Once a final method was chosen, it was used to generate a live load distribution for each condition. This chapter then describes how these distributions were used to calculate shears and moments in the box culvert. These shears and moments were then used to generate a uniform live load that would produce the same maximum shear or moment, whichever was critical.

3.1 Live Load Pressure Calculations

Each of the methods described in Section 2.2 was used to calculate the pressure due to a live load at the surface for a given depth of fill and compared with the results for the AASHTO method. The goal for this portion of the research was to compare other methods of live load calculation to the AASHTO method for calculating live loads and to determine if any of the other methods described here could be suitable alternatives.

3.1.1 Boussinesq Point Loads

The first method used to calculate the pressure increase was the Boussinesq point load method. For this and the other methods used, both the design tandem and design truck geometry were used. The design tandem consisted of two 25-kip axles, with a 4 ft axle spacing. The design truck geometry consisted of two 32-kip axles with a variable spacing of 14 ft to 30 ft. For both, the wheel spacing was 6 ft. Also, the driving axle was neglected because its load was much lower than the rear axles, therefore its contribution would have been negligible. The tire footprint was 20 inches wide by 10 inches in length. After checking results from various axle spacing, it was determined that the 14 foot spacing would produce the most critical pressures and therefore was used for all subsequent calculations involving the design truck geometry. In addition to the original Boussinesq calculations, which were for one tandem or truck only, additional load conditions of two loaded lanes were calculated. This was done for both the design tandem and the design truck geometries. Therefore there were four possible load conditions: tandem one lane, tandem two lane, truck one lane and truck two lane.

For each condition, a grid was set up in the longitudinal direction of the truck (transverse with respect to the culvert). The pressure from only one of the wheels was calculated at each point. Due to symmetry, the total pressure at any point in the grid from all four wheels can be found by adding the pressures from the different points on the grid that correspond to the distances that the point in question is away from the other three wheels. For the one loaded lane conditions, all four wheels are from the same truck. However, for the 2 loaded lane conditions, the top 2 wheels are for one truck in one lane, and the bottom 2 wheels are for the truck in the second lane. It was assumed that the trucks in the 2 lanes were 2 ft apart. It was also assumed that the wheels farthest away from the second truck could be ignored because the maximum pressures would be found in the area where the 2 trucks were closest. Depths of fill from 2 ft to 12 ft were used. This method was used for all the other pressure calculations. The four loading conditions as well as the grid used for the pressure calculations are shown below in Figure 3-1 to

Figure 3-5. Figure 3-1 shows the tire contact area in respect to a truck axle, and is representative of the rectangles used in the other figures to denote the tire contact area. The dots shown indicate where pressures were calculated. The dots only extend in one direction past the tires, because due to symmetry, the pressures on the left side of the tire would be the same as the ones on the left. For the truck conditions, only points shown on the inside of the tires are shown. For points outside the tires, pressures at similar distances inside the tires were used because for the distance between the axles used, the contribution of the far tires was assumed to be insignificant.

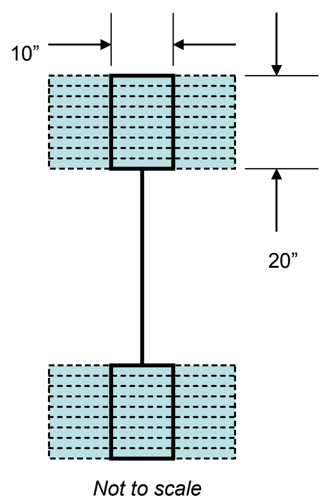

Figure 3-1. Tire contact area

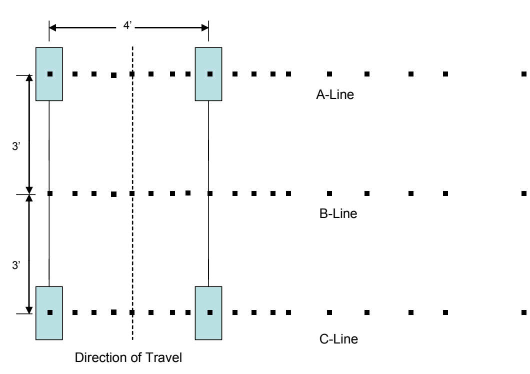

Figure 3-2. Tandem with 1 loaded lane

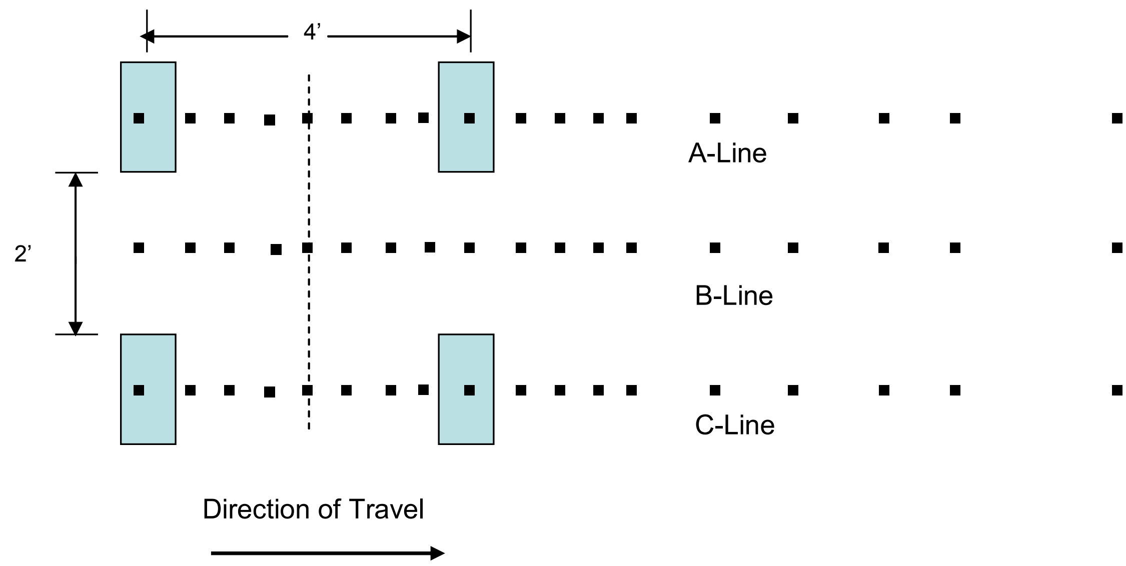

Figure 3-3. Tandem with 2 loaded lanes

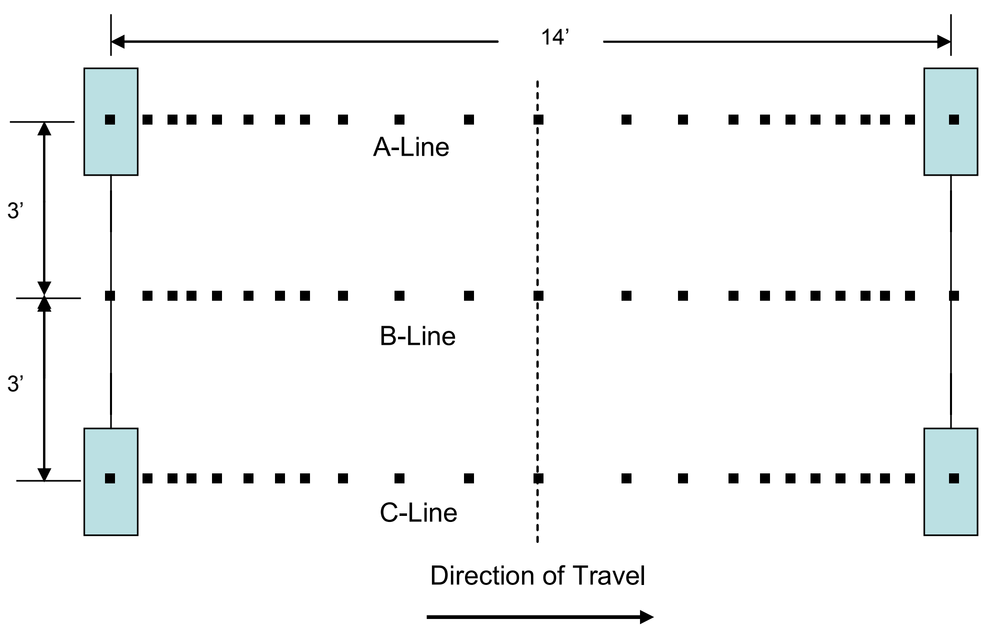

Figure 3-4. Truck with 1 loaded lane

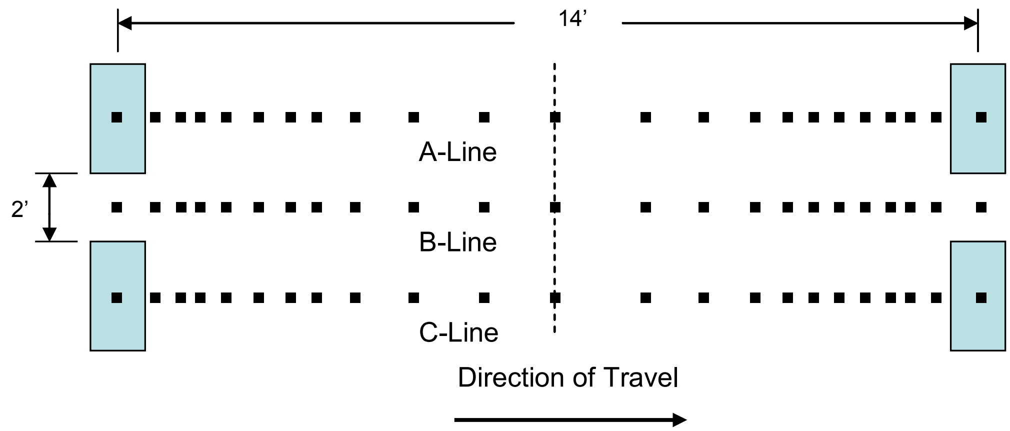

Figure 3-5. Truck with 2 loaded lanes

Equation 1-1 was used to calculate the pressures for this method. The results from the Westergaard equation (Eq. 1-2) were compared to those of Eq. 1-1, with the results from Eq. 1-1 predicting a slightly higher pressure increase. Therefore it was chosen over the Westergaard solution. For shallow depths of fill, the peak pressure was found to exist underneath the wheel loads, however, at greater depth, the peak pressure was found to be at points in the center of the axle and wheel spacing. When plotting distributions in the longitudinal direction, the peak pressures were taken for each depth, whether they were below the wheel loads, or in the center of the wheel spacing. For the tandem, at depths of fill of 4 ft and less, the pressure distribution exhibited two distinct peaks directly beneath the wheels. These distributions followed along the A-Line and C-Line shown in Figures 3-2 and 3-3. However, at depths of 5 ft and greater, the two peaks below the wheels were replaced with a single peak at the center of the axle spacing. These distributions followed along the B-Line as shown in Figures 3-2 and 3-3. For the truck, the peak was always under the wheels, regardless of depth. Results from the Boussinesq calculations can be seen in Figures 3-6 to 3-9.

3.1.2 Superposition

The next method of pressure calculation completed was the superposition method. As described above, this method is the integration of the Boussinesq solution over a rectangular loaded area. A similar grid system to the Boussinesq was used for this method as well, as well as the same test depths.

The pressure distribution at each depth followed the same pattern for each depth that the Boussinesq results did. Also, as the depth increased, the superposition results matched very closely to the Boussinesq results. This was expected because the superposition method is based on the Boussinesq equation. However, at shallow depths the difference between the results was significant. The Boussinesq equation predicted much higher pressures than the superposition method. The shallow depths of fill are the most critical situations, therefore being conservative is important. However, it is believed that the pressures from the Boussinesq are overly conservative due to the assumption that the load at the surface is a point load. The superposition method takes the actual loaded area, and is shown to be effective by its comparisons with the Boussinesq solutions at depth. Also, the patterns found in the superposition results matched the patterns found in the field loadings described in the previous chapter. The report from Texas A & M included a table of measured pressures from truck live loads. Although the axle loads and orientations were slightly different than those studied here, the results for the measured pressures were comparable to the computed ones. Table 3-1 shows this comparison. The table only shows the peak pressure at each depth. The two results match best at depths of 6 ft and greater, with the difference becoming larger with shallow depths. It is therefore important to be conservative at shallow depths based on this comparison. Therefore, the

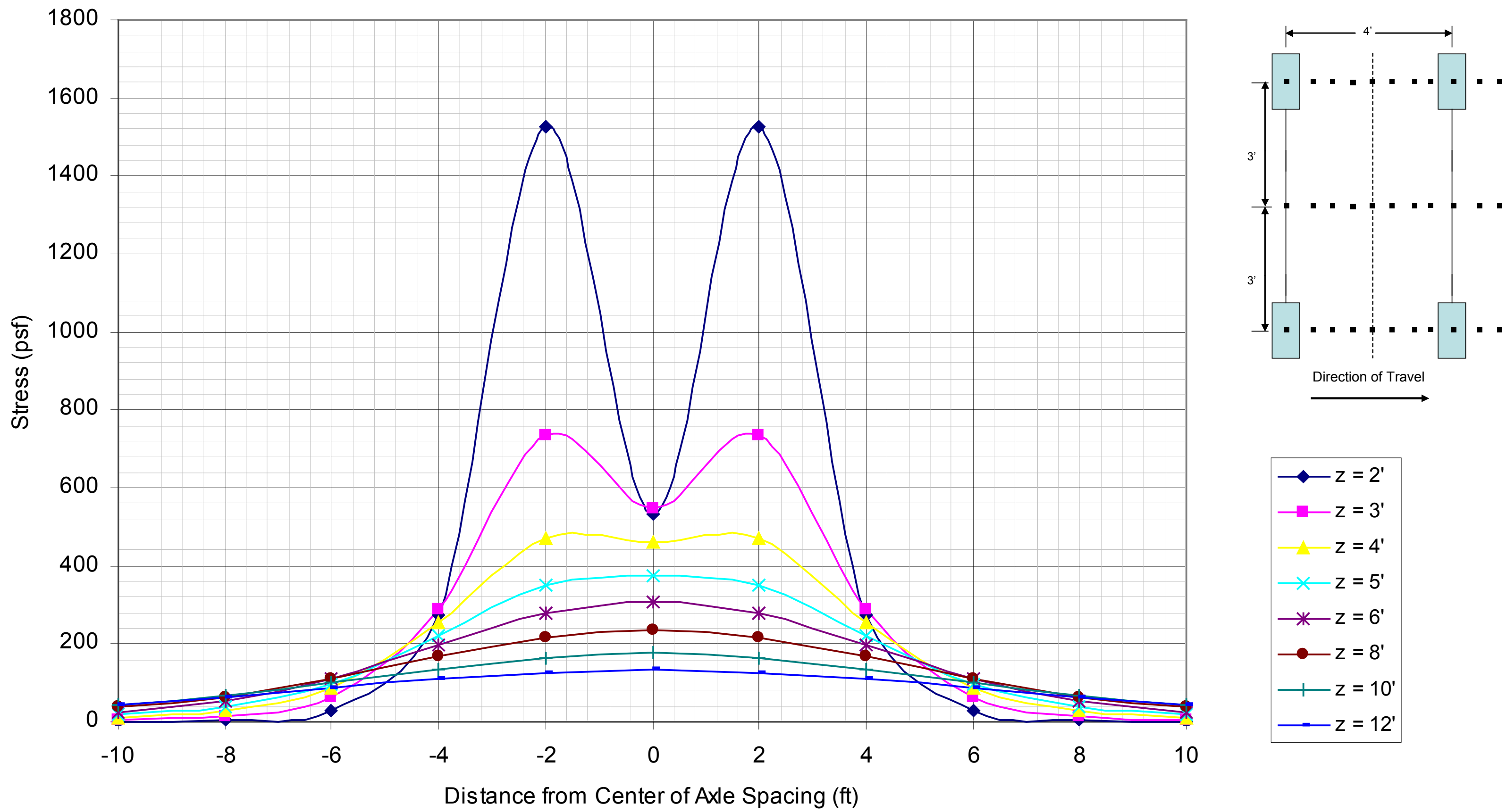

Figure 3-6. Boussinesq longitudinal pressure distribution, tandem, one loaded lane

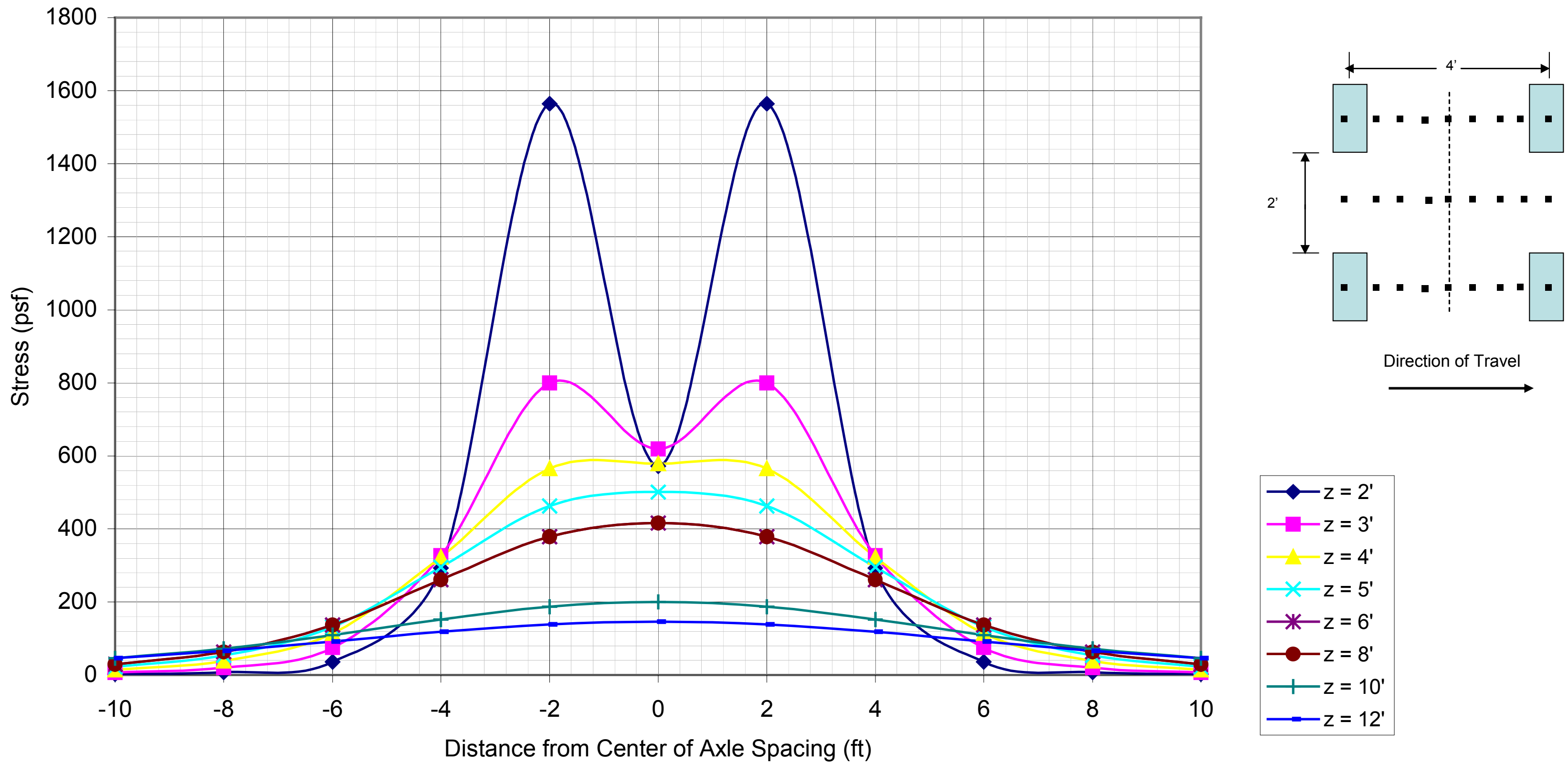

Figure 3-7. Boussinesq longitudinal pressure distribution, tandem, two loaded lanes

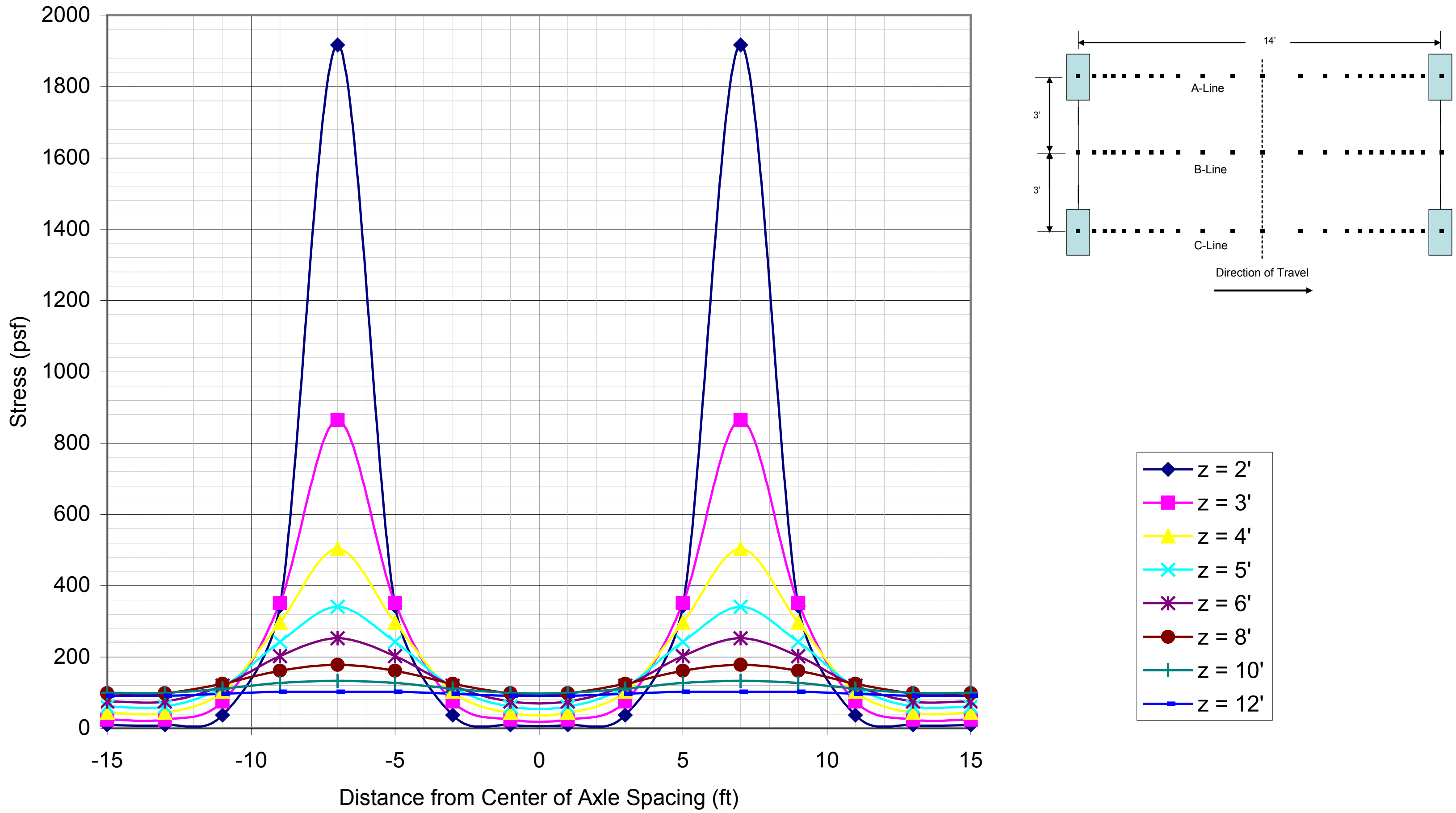

Figure 3-8. Boussinesq longitudinal pressure distribution, truck, one loaded lane

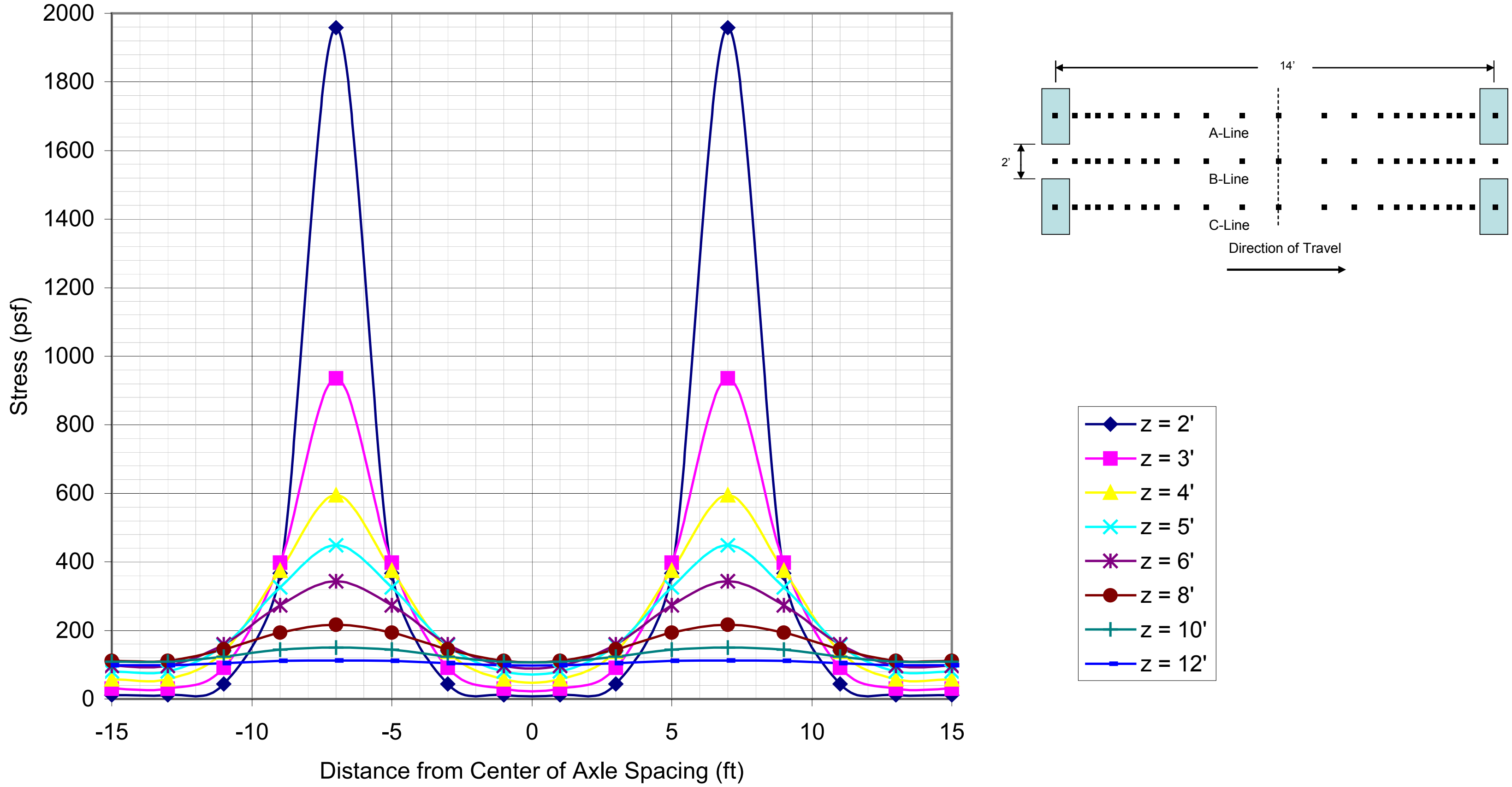

Figure 3-9. Boussinesq longitudinal pressure distribution, truck, two loaded lanes

superposition method was selected as the more viable option for final pressure increase calculations. Results from the superposition calculations can be seen in Figures 3-10 to 3-13.

Table 3-1. Calculated pressures versus measured pressures (tandem)

Depth (ft)	Superposition peak pressure (psf)	Superposition peak pressure (psi)	Measured peak pressure (psf)	Measured peak pressure (psi)
2	1300	9.0	1901	13.2
4	453	3.1	590	4.1
6	307	2.1	274	1.9
8	234	1.6	274	1.9

Measured pressures are from a TAMU study done in 1984 [7]
Calculated Pressures are one calculated using the superposition method
The TAMU pressures used 24 kip axles
The superposition method used 25 kip axles

3.1.3 Buried Pipe

For the buried pipe method of pressure calculations, the same depths of fill were used as in the previous calculations. This method did not require the loading grids as did the previous methods, however it required the dimensions of the culvert to be used as inputs, therefore the initial selections of a 12’ x 12’, 10’ x10’, 8’ x 8’ and a 6’ x 6’ culvert cross sections were used.

With the exception of the 2 ft of fill condition, this method produced the lowest pressures due to the live load. In addition to the inherent limitations of the method based on its origin, there were other problems with this method. First is the fact that the culverts dimensions play an integral role in the calculations. It would be difficult to implement this method into a standardized practice because new load coefficients would have to be determined based on each culvert’s geometry. This problem would not be as imposing if not for the fact that the load coefficients are in table form and are not an equation. Also, for the small number of culvert sizes tested here the limits of the table of coefficients was reached. These size culverts, which are believed to be common sizes, produced situations where the limiting value had to be used, which could greatly compromise accuracy. In light of these limitations, this method was not further investigated and is not recommended in box culvert applications. Results from these calculations can be found in Table 3-1 in the following section as well as in Appendix A.

3.1.4 AASHTO

The above calculations were compared to the results from the current LRFD AASHTO method of calculating the pressures at depth from a live load at the surface. As described above in Section 2.2.4, the AASHTO method involves taking the surface loaded area and increasing its dimensions on both sides by a factor of 1.15 times the depth of fill. Portions of the FDOT Mathcad Box Culvert Design program were used to calculate the AASHTO pressures. With the exception of the 2 ft of fill condition, the AASHTO method returned pressures higher than the superposition method. The difference between the AASHTO and superposition results was not too great to question the validity of either set of calculations, but large enough that the use of the superposition method could result in designs that are conservative, but not overly conservative. The results from all pressure calculations are shown below. For comparison purposes, only the maximum pressure for each depth is shown here. In general, the 2 loaded lane truck conditions produced the largest pressures at shallow depths, while the 2 loaded lane tandem conditions produced the largest pressures at larger depths (5 ft and greater).

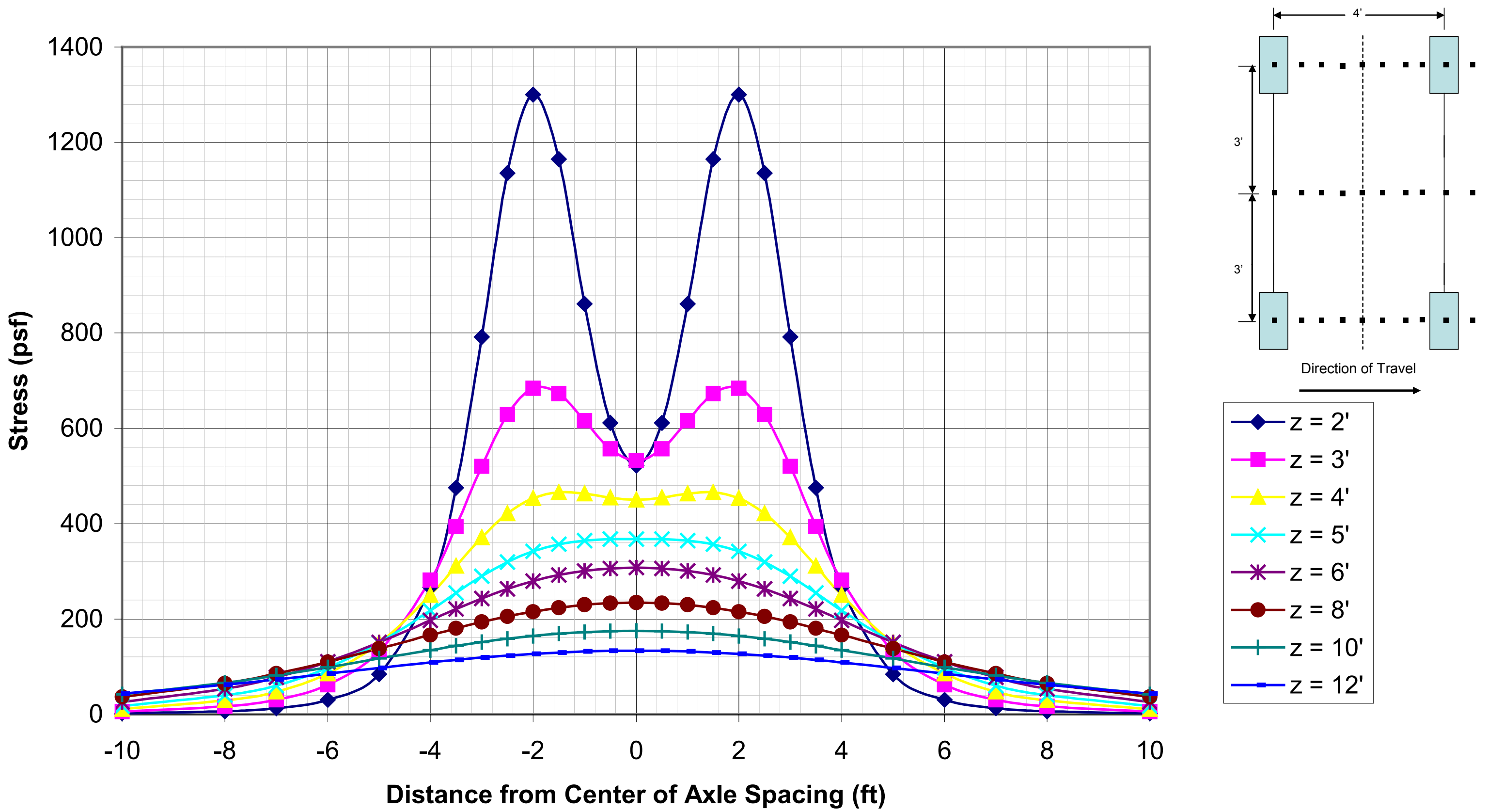

Figure 3-10. Superposition longitudinal pressure distribution, tandem, one loaded lane

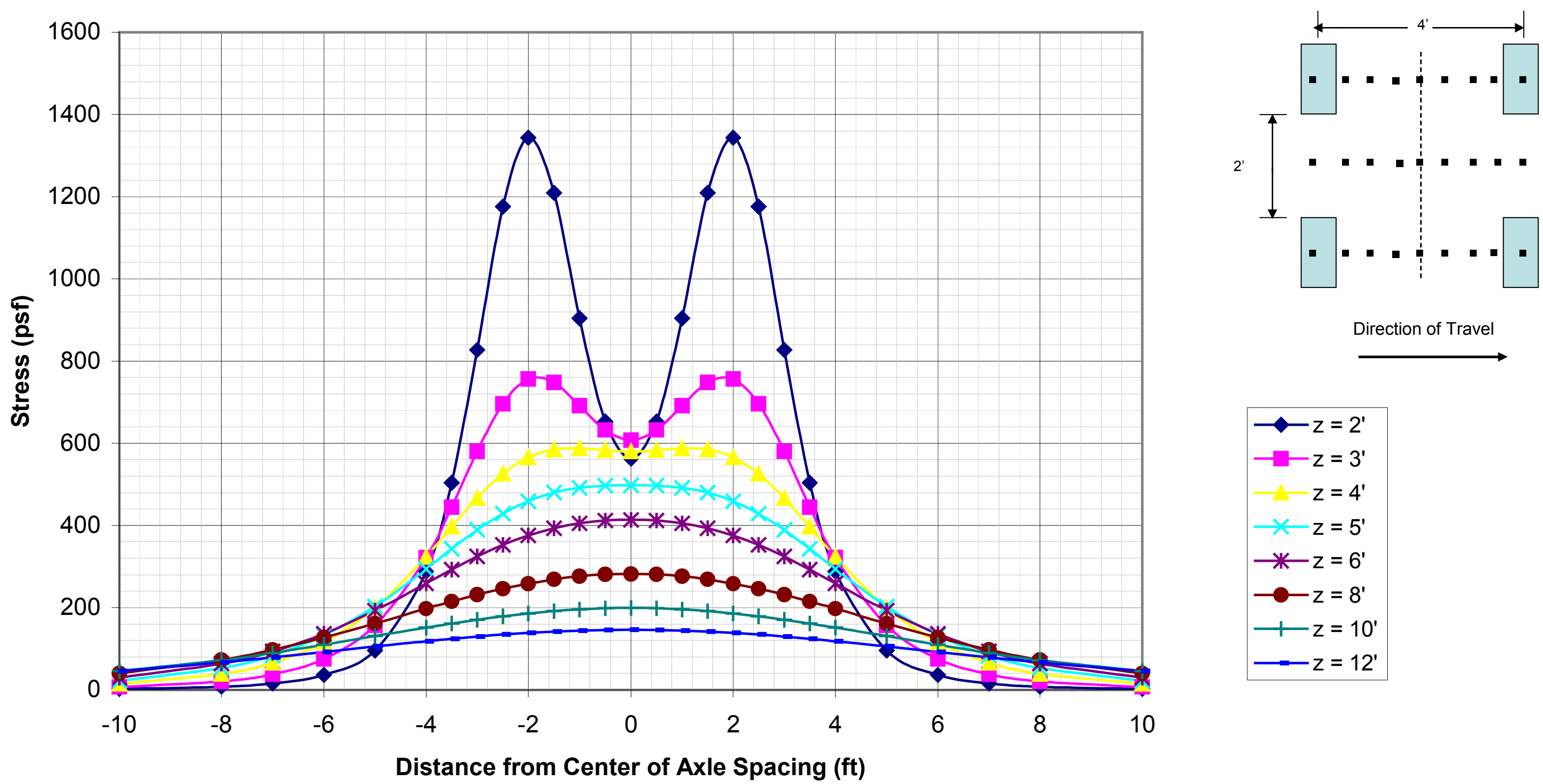

Figure 3-11. Superposition longitudinal pressure distribution, tandem, two loaded lanes

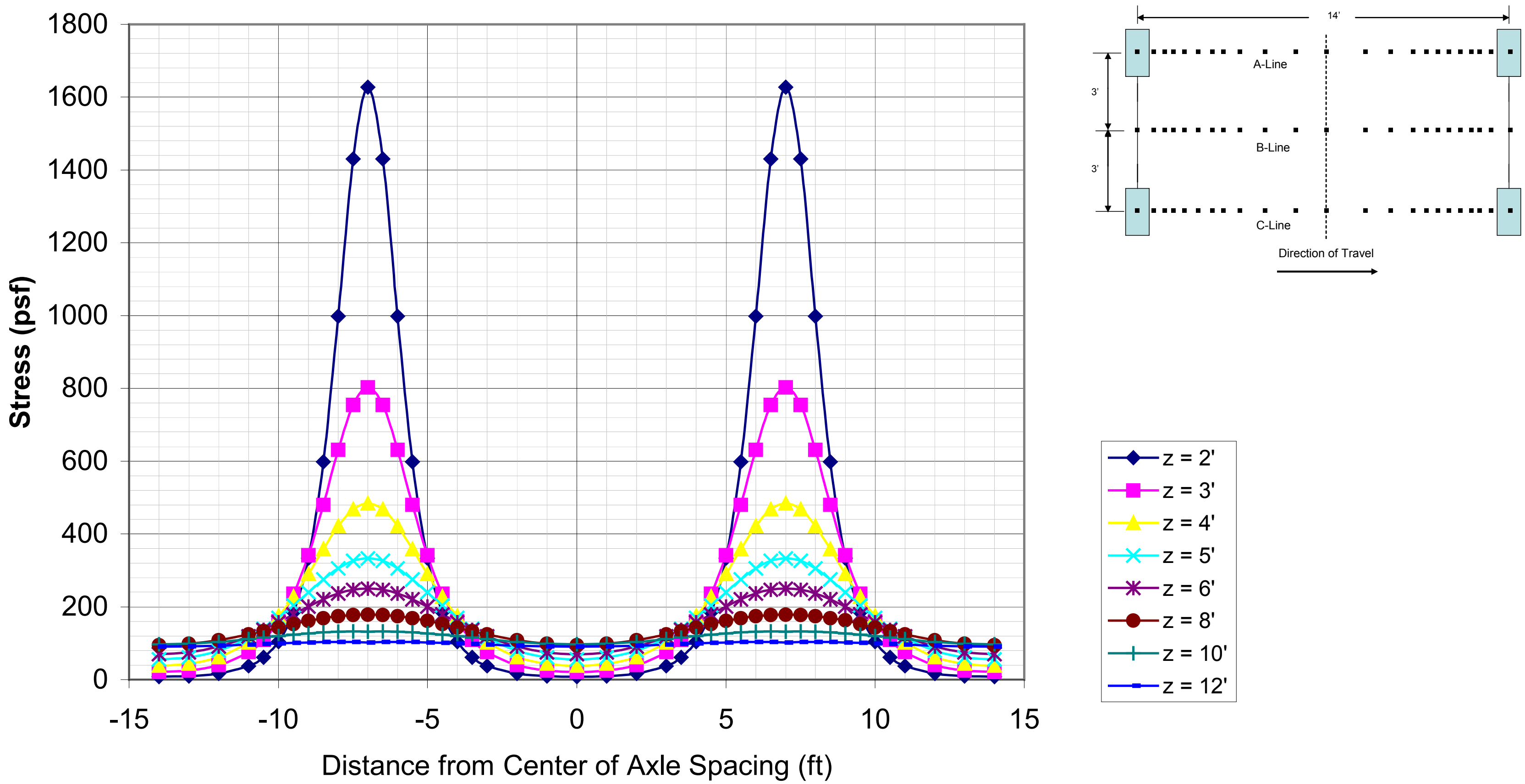

Figure 3-12. Superposition longitudinal pressure distribution, truck, one loaded lane

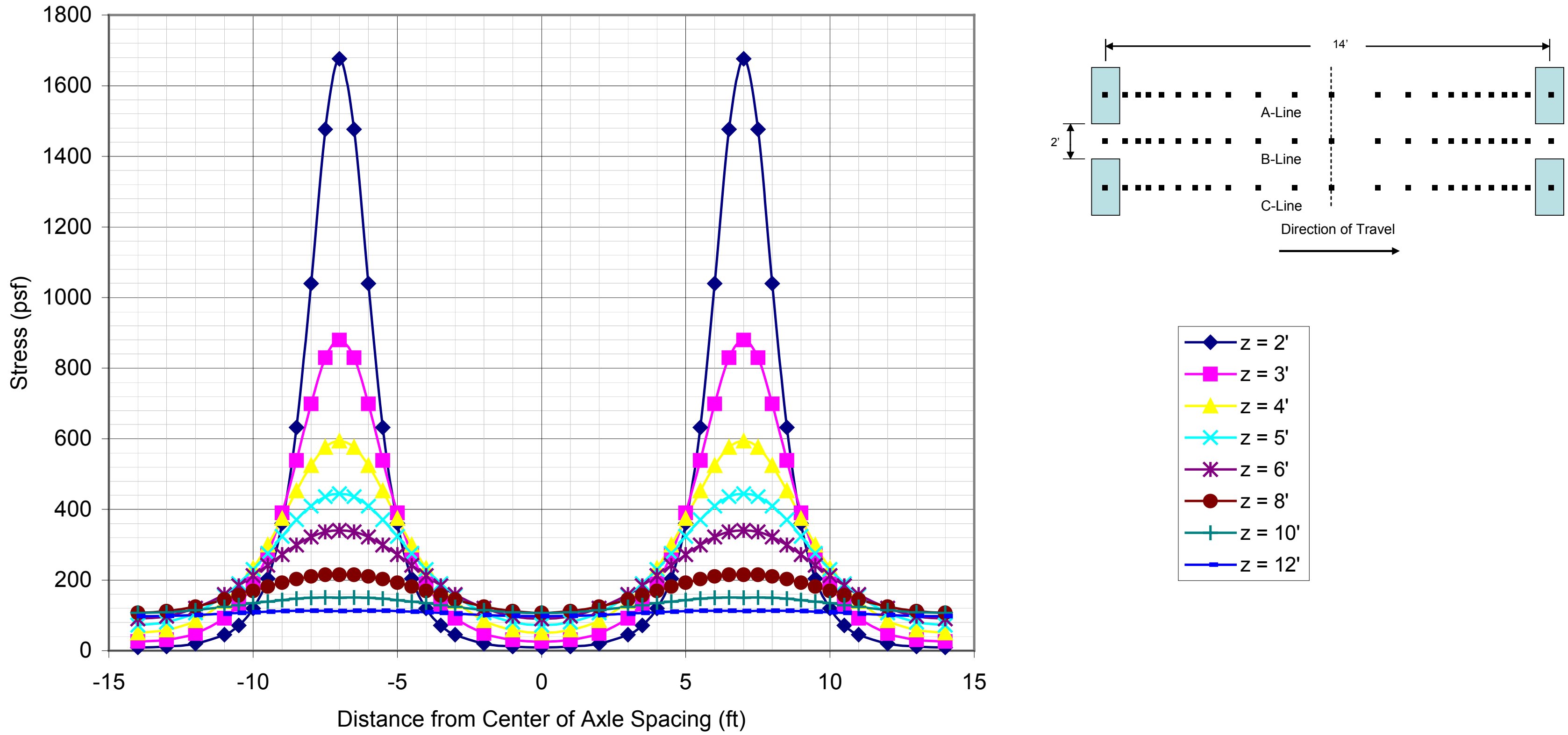

Figure 3-13. Superposition longitudinal pressure distribution, truck, two loaded lanes

The AASHTO specification states that this maximum pressure be applied to the entire loaded area for any given depth, as was shown in Figure 2-4. Therefore, only the maximum pressures are shown here. Pressures are shown in psf. Impact was not accounted for in these pressures. Complete results of all calculations can be found in the Appendix A.

Table 3-2. Peak pressure comparison

Depth (ft)	Peak pressure 1 loaded lane (psf)			
	Boussinesq	Superposition	Buried pipe	AASHTO
2	1526	1300	1574	1208
3	732	684	672	708
4	469	453	340	476
5	373	342	267	404
6	306	307	227	347
8	234	234	177	265
10	176	175	171	210
12	134	133	171	171

Depth (ft)	Peak pressure 2 loaded lanes (psf)			
	Boussinesq	Superposition	Buried pipe	AASHTO
2	1958	1676	1574	1546
3	936	879	672	876
4	594	593	340	576
5	501	498	267	435
6	416	413	227	341
8	284	282	177	237
10	200	198	171	178
12	146	145	171	142

NOTE: Buried Pipe Method does not account for 1 or 2 lanes, therefore no change.

Based on the results of all the pressure calculations, the superposition method was chosen to be the method used in place of the AASHTO method of calculating the pressures due to a live load at the surface. It produces credible results, which are slightly less than the current AASHTO method. Also, the distribution from the superposition results produces a much more realistic scenario that the current AASHTO methodology of distributing the maximum pressure over the entire loaded area.

3.2 Shear, Moment, and Equivalent Loads

3.2.1 Process/Ideology

Once a method for calculating the pressure at a given depth was selected, the next step was to find what shears and moments the loading would generate in the box culvert, and what uniformly distributed load would produce the same shears and moments. First, some assumptions had to be made about the box culvert system. The first assumption was that the top slab of the culvert was simply supported. This assumes that the connection between the top slab and the walls can carry no moment, and behave as a pinned connection. This is often not the case in reality, some moment would be generated in the corners of the culvert, but for simplicity and for conservativeness, this resistance was neglected. Also, the pressures calculated have the dimensions of load divided by length squared. Distributed loads on beams are taken as load per length. Therefore, the top slab of the box culvert was assumed to have a unit width of one foot. This would automatically convert the pressures previously calculated to a load per foot dimension acceptable for shear and moment calculations. In this way, a uniformly distributed live load can be found to use as a design live load for a given depth of fill. This is also conservative because it assumed that there was no dissipation of the load in the direction transverse to the direction of the truck. In reality, the transverse distribution would be similar to the longitudinal one.

The process began by using the load distributions shown in Figures 3-10 to 3-13 on the top slab of the box culvert. The data points were connected with straight lines to form trapezoids. Depending on the span length in question, different sections of the load distribution were taken. Spans of 6, 8, 10, 12, and 14 ft were used. These spans were selected because it is believed that the majority of box culverts used are within those dimensions. For the tandem conditions, it was found that the section of the load distribution that produced the peak load was the section under the center of the axle spacing, as shown in Figure 3-14, as opposed to sections on the end of the distribution, as shown in Figure 3-15. The two peaks in Figure 3-14 relate to the location of the tires. For the truck conditions, the section of the load distribution centered between the 2 axles wasn't used because due to the large distance between them (14 ft) the loads there were very small. Figure 3-16 shows the typical distribution used in the truck conditions. Since both shapes of distributions (Figures 3-14 and 3-16) were symmetrical, this meant that the load distributions used for each span were symmetrical. The values of the data points (load and distance, x) were placed in separate arrays in Mathcad. The load distribution was broken into trapezoidal areas; the area of each individual trapezoid was calculated, as well as the distance from its center of gravity to one of the endpoints. Multiplying each individual trapezoid's area by its moment arm, summing those areas across the beam, and dividing by the span length found one of the reactions. The other reaction, due to symmetry, was found by subtracting the previously calculated reaction from the total area under the load distribution curve. The two reactions were the same for each case because of the symmetrical loading. This process is shown as Figure B-1 in Appendix B.

Next, knowing the load distribution and the reactions, the shears and moments were calculated. The shear at either end of the span was equal to the reaction. The subsequent values of shear along the span were found by subtracting the area of each trapezoid from the previous value of shear, starting with the left reaction. A shear diagram was produced in this way. Moments along the span were calculated in the same manner.

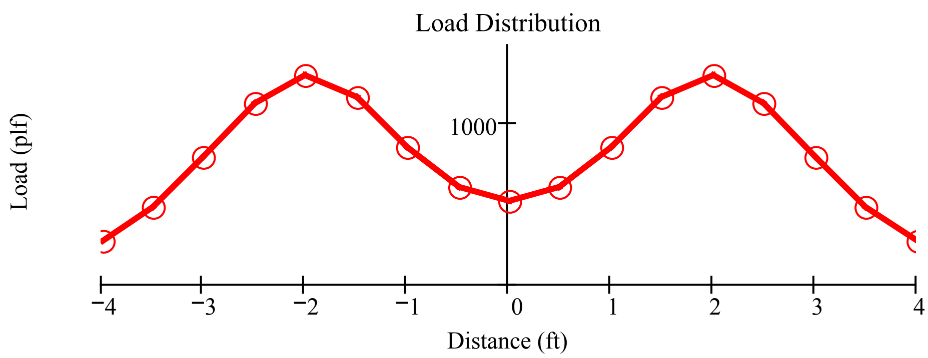

Figure 3-14. Sample load distribution under the center of tandem axle spacing

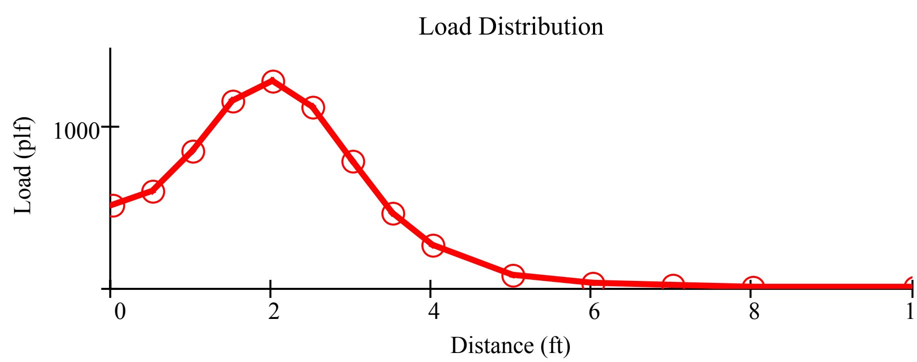

Figure 3-15. Sample load distribution under the end of the tandem distribution

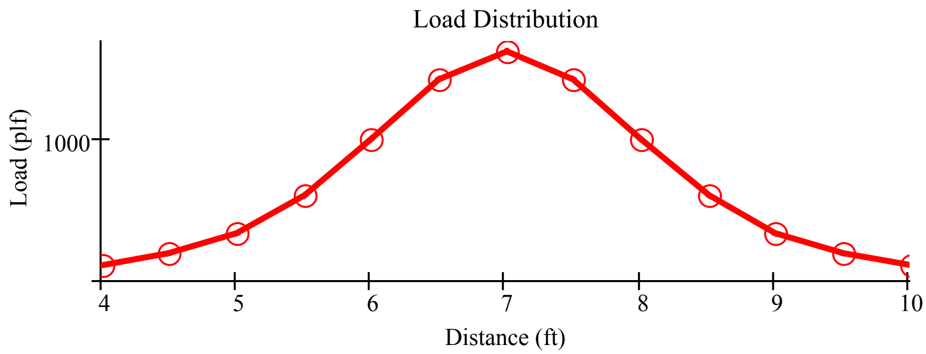

Figure 3-16. Sample load distribution under wheel for truck distribution

Because the span was modeled as simply supported, the moments at each end were zero. Then by adding the area under the shear diagram, the moments could be found. Area was added to generate a positive moment. It could have been subtracted with the same results, only the sign would be negative. Positive moments were chosen for simplicity.

By knowing the maximum shear and the maximum moment, an equivalent load could be calculated. Two equivalent loads were calculated, one based on the maximum shear and one based on the maximum moment. By having a simply supported beam, the equivalent load (q) based on shear (V) could be found by solving for q in the equation $V=ql/2$. Similarly, the equivalent load based on the maximum moment (M) was found by solving for q in the equation $M = ql^2/8$. It was found that for most load cases the equivalent load based on the maximum moment was larger than the one based on shear. The only exceptions were for the 6 foot spans, at depths of 2 and 3 ft, for the 1 and 2 loaded lane tandems. A sample pressure distribution and the equivalent uniformly distributed load that produces the same maximum moment are shown in Figure 3-17.

3.2.2 Equivalent Load Results

For each of the four load scenarios, depth of fill and span length, an equivalent uniformly distributed load was found. A few patterns emerged from the data collected. First, as the depth of fill was increased, the equivalent uniform decreased. This result was expected because as more soil is added above the culvert, the load is further dissipated. Another pattern was that for a given depth of fill, the equivalent load decreased slightly as the span was increased. When solving for the load q, as the length increases, the moment is being divided by a larger and larger number, so it is expected that the equivalent load decreases with an increase in span length. Also, for larger spans the peak load is occupying a smaller percentage of the total length, therefore this reduction in the equivalent load is expected. At larger depths, the change in load with span was very small. For the truck scenarios, the reduction in equivalent load with span length was dramatic at shallow depths (2 and 3 ft of fill). However, with increasing depth, the spans influence on the equivalent uniform load is diminished. The Figures 3-18 to 3-21 show the equivalent loads for each condition, depth of fill and span length. A complete table of results can be found in Appendix B.

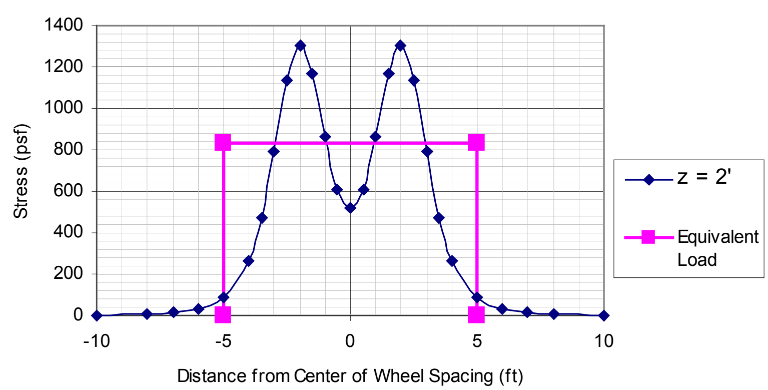

Figure 3-17. Sample pressure distribution and equivalent load for tandem, 1 lane, 2’ of fill and 10’ span

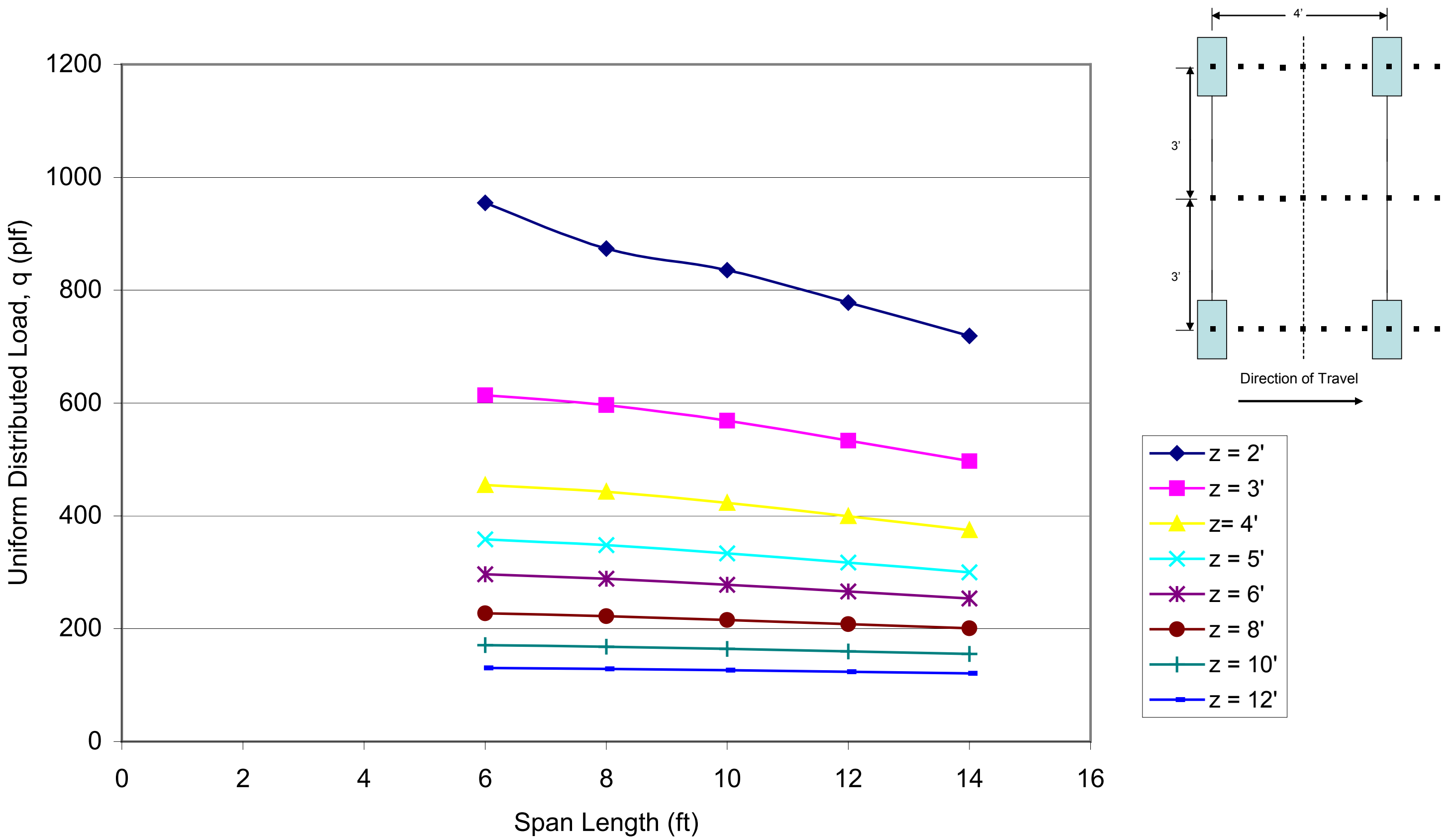

Figure 3-18. Uniform distributed load vs. span length – tandem, 1 loaded lane

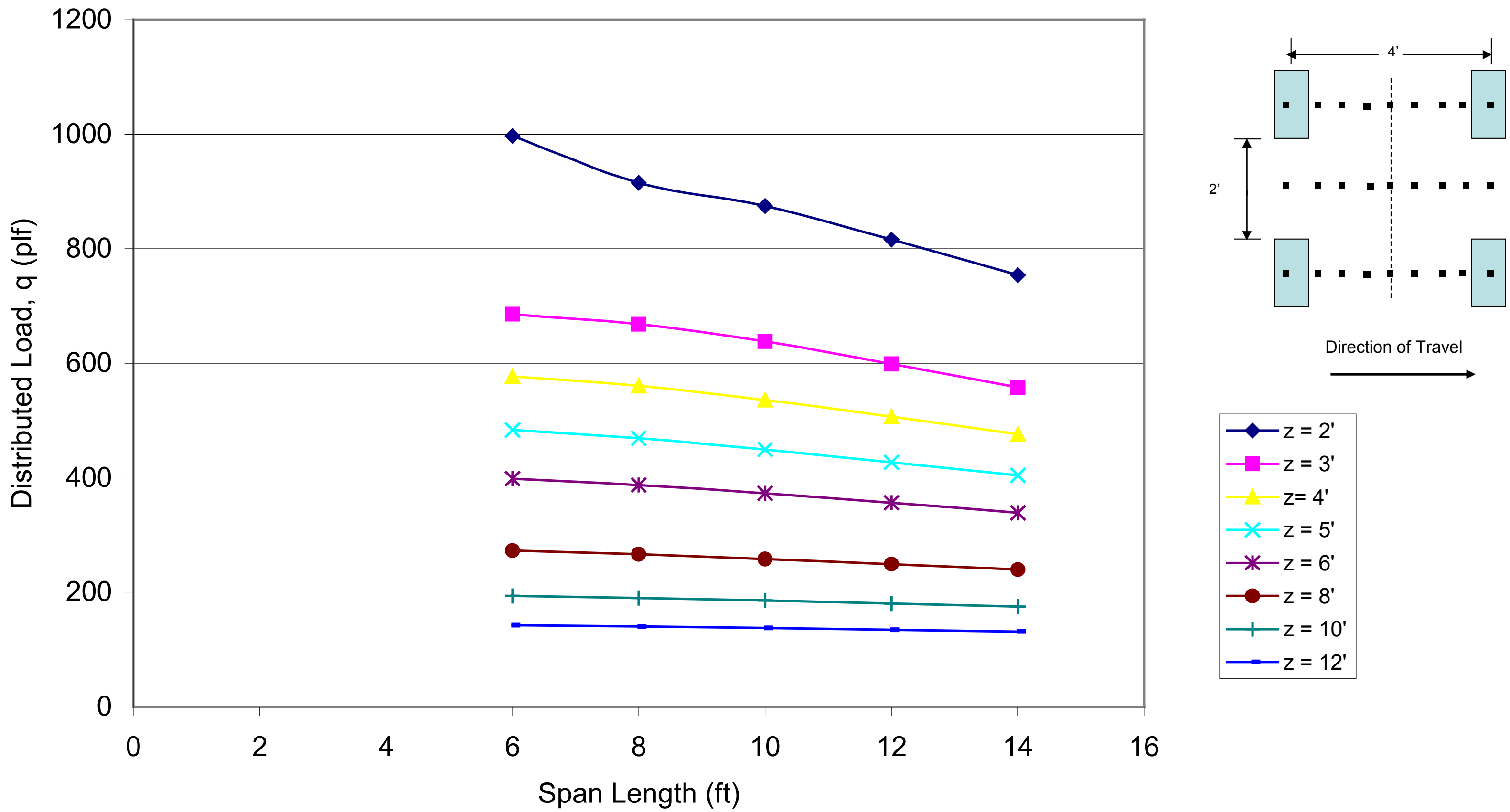

Figure 3-19. Uniform distributed load vs. span length – tandem, 2 loaded lanes

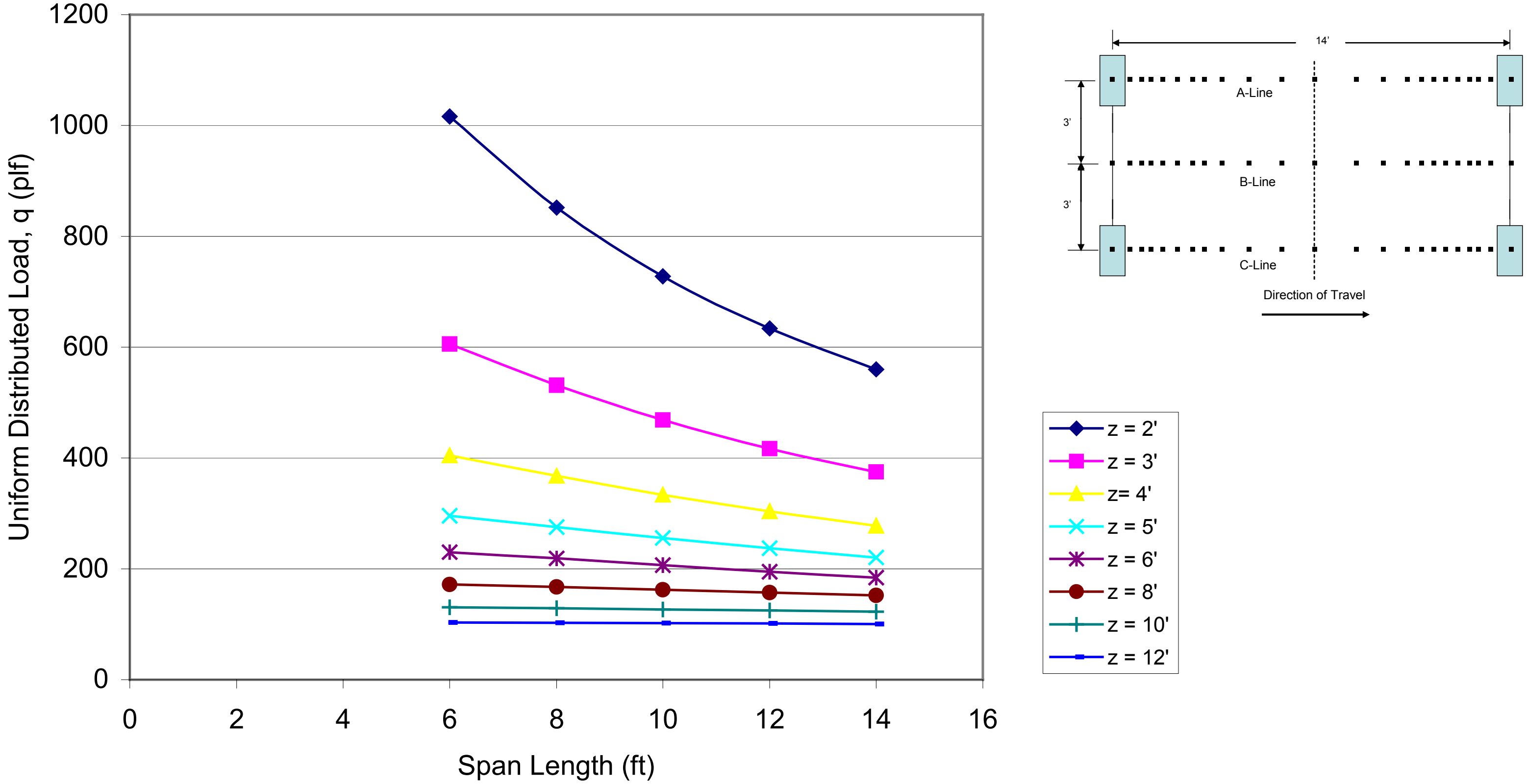

Figure 3-20. Uniform distributed load vs. span length – truck, 1 loaded lane

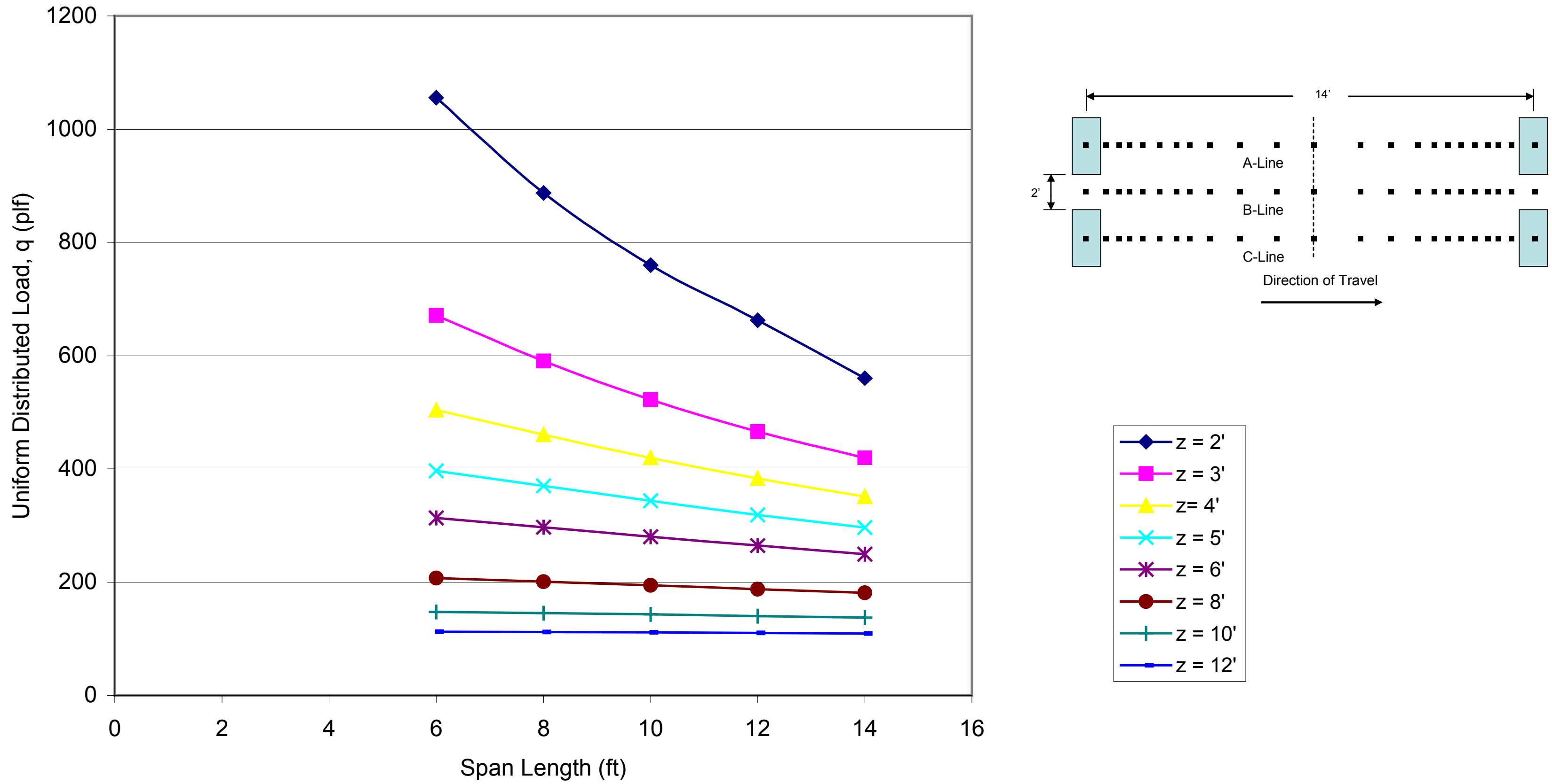

Figure 3-21. Uniform distributed load vs. span length – truck, 2 loaded lanes

CHAPTER 4
CURVE FITTING

This chapter describes how equations were found that model the patterns that the equivalent uniform live loads follow when compared to span length and depth of fill. An equation was found for each load condition. The final equation was the one that predicted the largest uniformly distributed equivalent load.

4.1 Live Load Design Equations

Once the equivalent loads for all possible combinations of loading, depth and span length were calculated, the final goal was to determine if an equation could be found that would predict the same equivalent loads based on either the span and depth, or the depth of fill only. Because of the fact the equivalent load changed very little with a change in span for most depths of fill (greater than 3 ft), it was suggested that the model equation be independent of the culvert's span. Therefore, only the maximum equivalent load was taken for each depth. For the both the tandem and truck conditions, this was for a 6 foot span. By neglecting the fact that increases in culvert span length generate a lower equivalent load, this method is conservative. For each of the four load conditions, the equivalent load was plotted against the depth of fill, and both linear and nonlinear regression was used to fit the data. The first set of equations shown below came from Excel's power series trendline function. This generated a set of four possible live load prediction equations (one for each load condition). These equations are listed below as Equations 4-1 to 4-4. In the following equations, q is the equivalent uniform load, and z is the depth of fill.

- $q = 1877.8*z^{-1.0522}$ (4-1)
- $q = 2339*z^{-1.06}$ (4-2)
- $q = 2398.1*z^{-1.2748}$ (4-3)
- $q = 2806.6*z^{-1.2741}$ (4-4)

A second program was used to compare the results from Excel. This program was called Curve Expert and used nonlinear regression to find its equations. Excel's power series results matched the calculated data well, so power series equations were used in the Curve Expert analysis. The results from this program are shown below.

- $q = 1999.5*z^{-1.068}$ (4-5)
- $q = 1907.8*z^{-0.9125}$ (4-6)
- $q = 2529.6*z^{-1.314}$ (4-7)
- $q = 2353.123*z^{-1.1425}$ (4-8)

These equations were then calculated for values of depth (x) from 2 to 12 ft. The results were then compared. The results from the two sets of equations match rather closely, and are shown along with the calculated data points in Figures 4-1 to 4-4. The Excel and Curve Expert results produced roughly similar style of equations. Equations 4-2 and 4-6 produced the largest loads, and pertain to the tandem 2 lane condition.

In order to be conservative, the final design equation was based on the condition that produced the largest loads. In most cases, the culvert would be under a road with 2 directions of traffic, so it would have been unreasonable to consider the one lane conditions because there would always be the opportunity for both lanes to be simultaneously loaded. The condition that produced the largest loads was the tandem with 2 loaded lanes condition (Table 4-1). Therefore it was suggested that the final design equation be based upon the data for that load condition. By basing the equation on the worst case condition, it would be conservative for all other conditions. Figure 4-2 shows the best-fit curve results for the tandem with 2 loaded lanes condition. Equation 4-2 matched the calculated data much better than Equation 4-6 for most depths of fill. Equation 4-2 produced loads that were slightly lower than the calculated data at depths of 10 ft and greater. However, at those depths, the load is small and this small difference can be considered negligible. For ease of use, Equation 4-2 was simplified in order to produce the final design equation. The recommended design equation is shown as Equation 4-9.

$$q = \frac{2300}{z} \tag{4-9}$$

The use of equation 4-9 is recommended because it produces live loads that are similar to the calculated values for the worst case (tandem with 2 loaded lanes). Table 4-1 compares the calculated values to the values from Equation 4-9. This data is also presented in Figure 4-1.

Equation 4-9 would not be suitable for depths of fill 2 ft or less, as prescribed by the AASHTO specification. The AASHTO specification states that for depths of fill less than 2 ft, the effect of the fill on the distribution of the live load shall be neglected (AASHTO). Also, because Equation 4-9 was based on the shortest span studied, 6 ft, it is conservative. For spans less than 6 ft this equation is not applicable.

Table 4-1. Calculated live loads and design equation live loads

Depth (ft)	Uniform distributed load (q), plf				
	Tandem 1 lane	Tandem 2 lanes	Truck 1 lane	Truck 2 lanes	Eq. 4-9
	Calc	Calc	Calc	Calc	
3	614	686	606	671	757
4	454	577	405	504	560
5	358	484	296	396	443
6	296	399	230	313	366
7	---	---	---	---	311
8	227	273	172	207	270
9	---	---	---	---	239
10	171	194	131	148	214
11	---	---	---	---	194
12	131	143	103	103	177

Note: --- indicates where data was not calculated

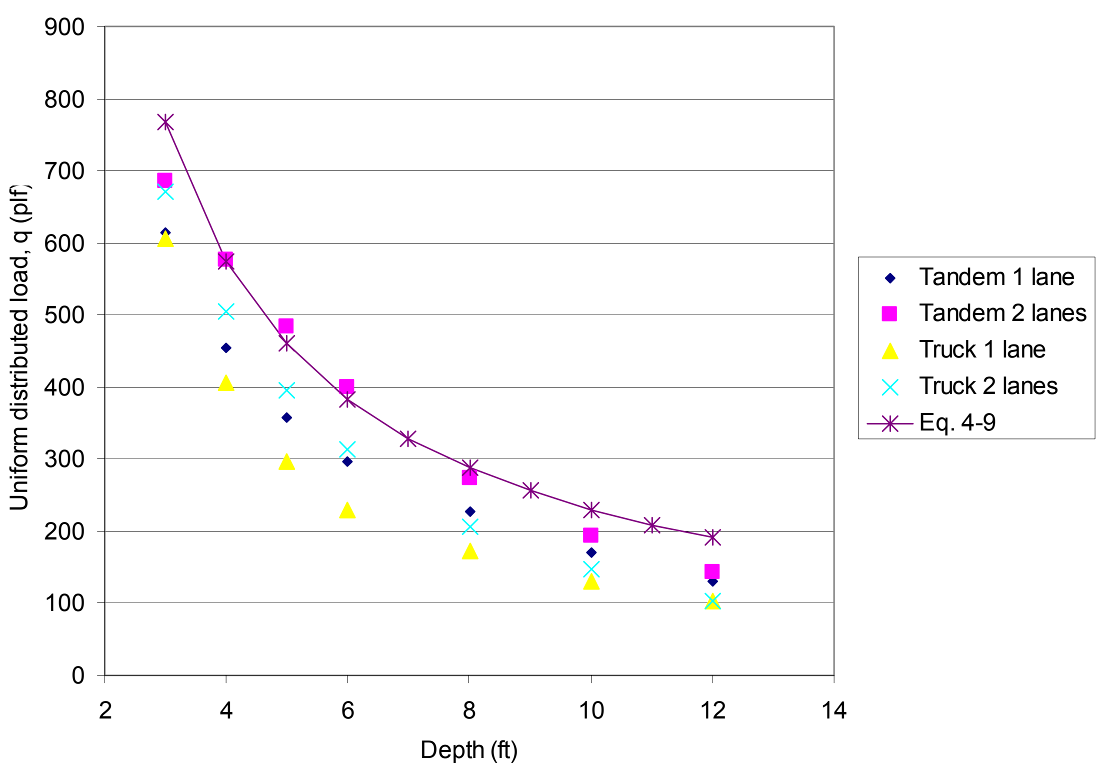

Figure 4-1. Calculated live loads and design equation live loads

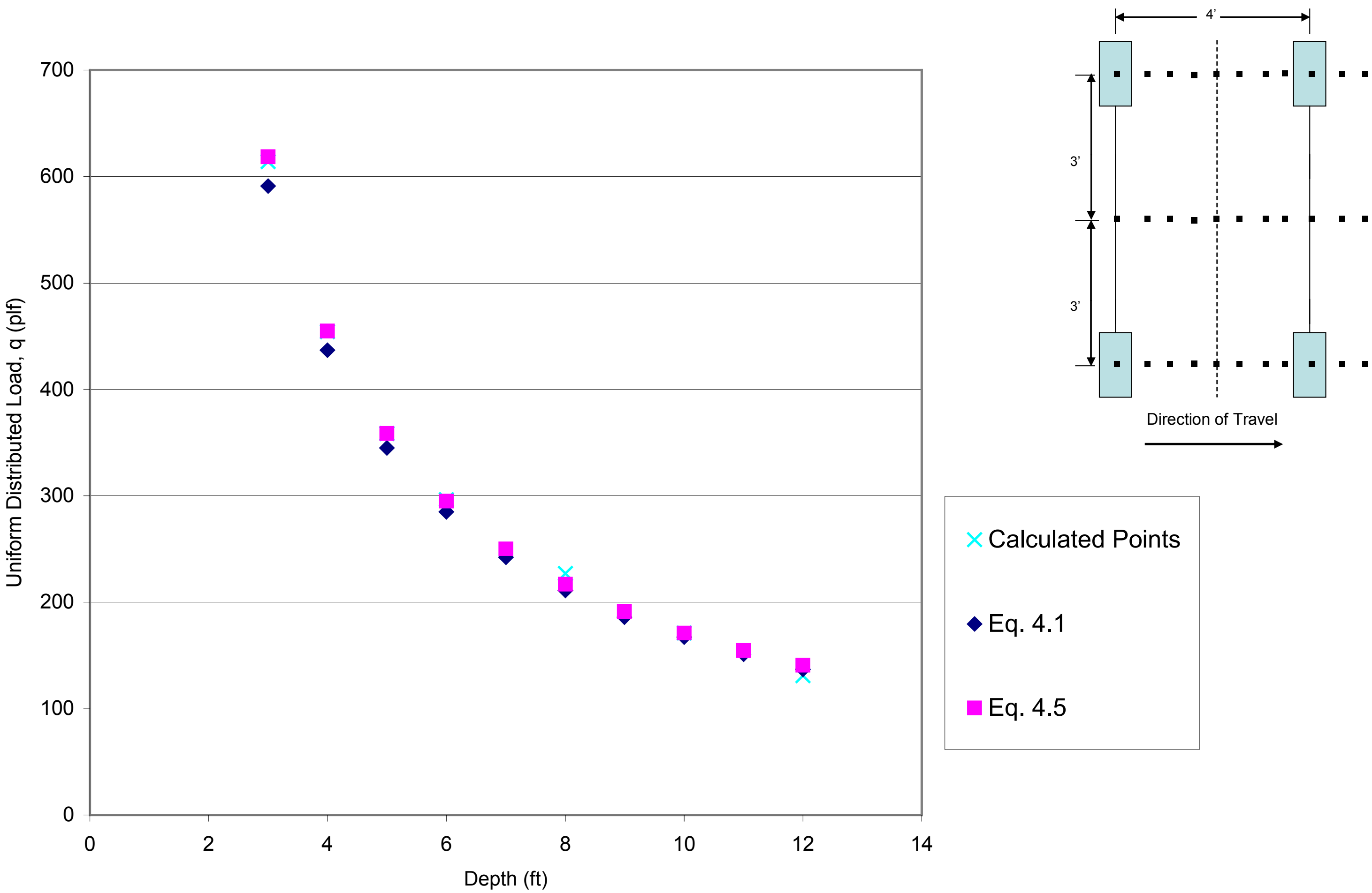

Figure 4-2. Best fit equation comparison – tandem, 1 loaded lane

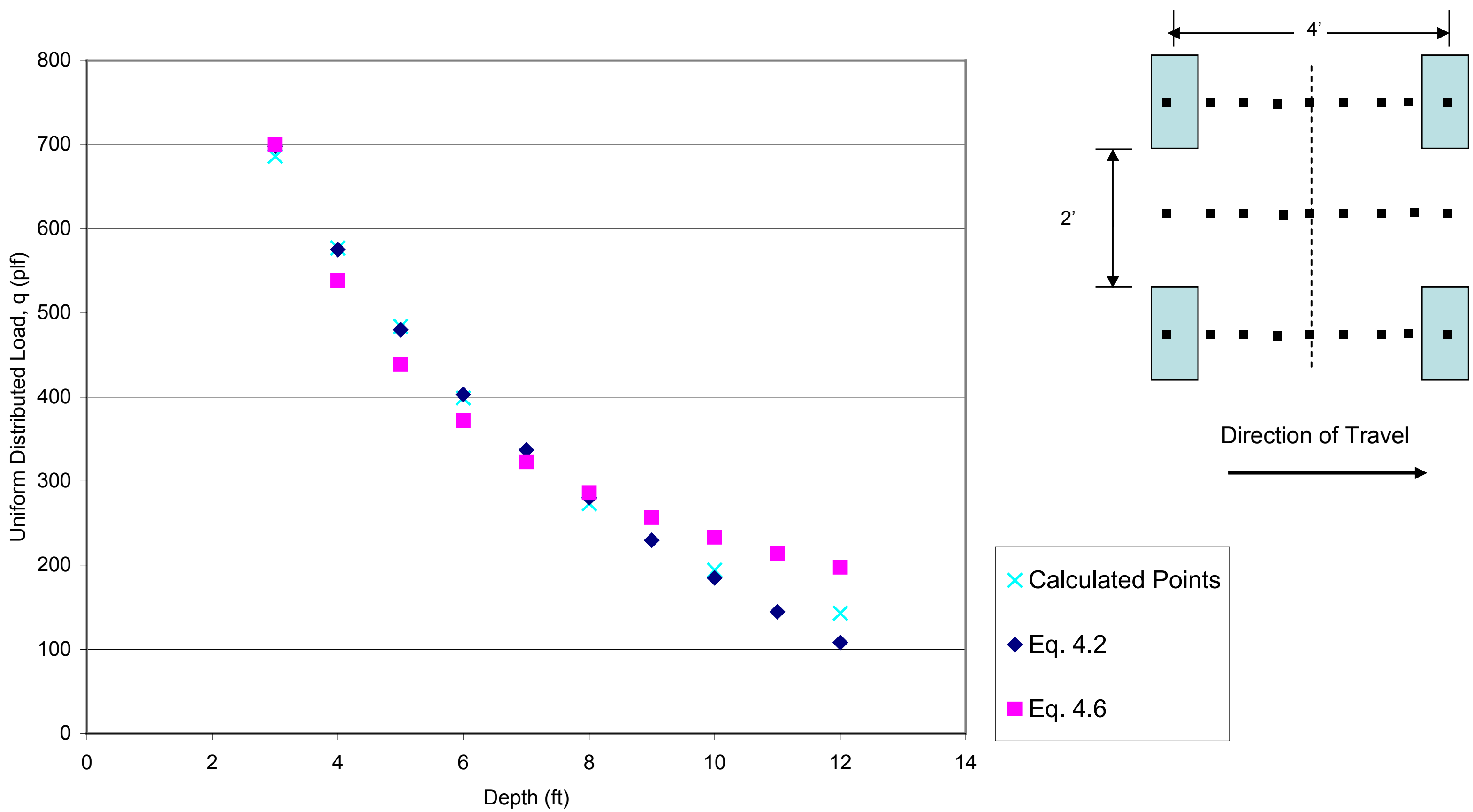

Figure 4-3. Best fit equation comparison – tandem, 2 loaded lanes

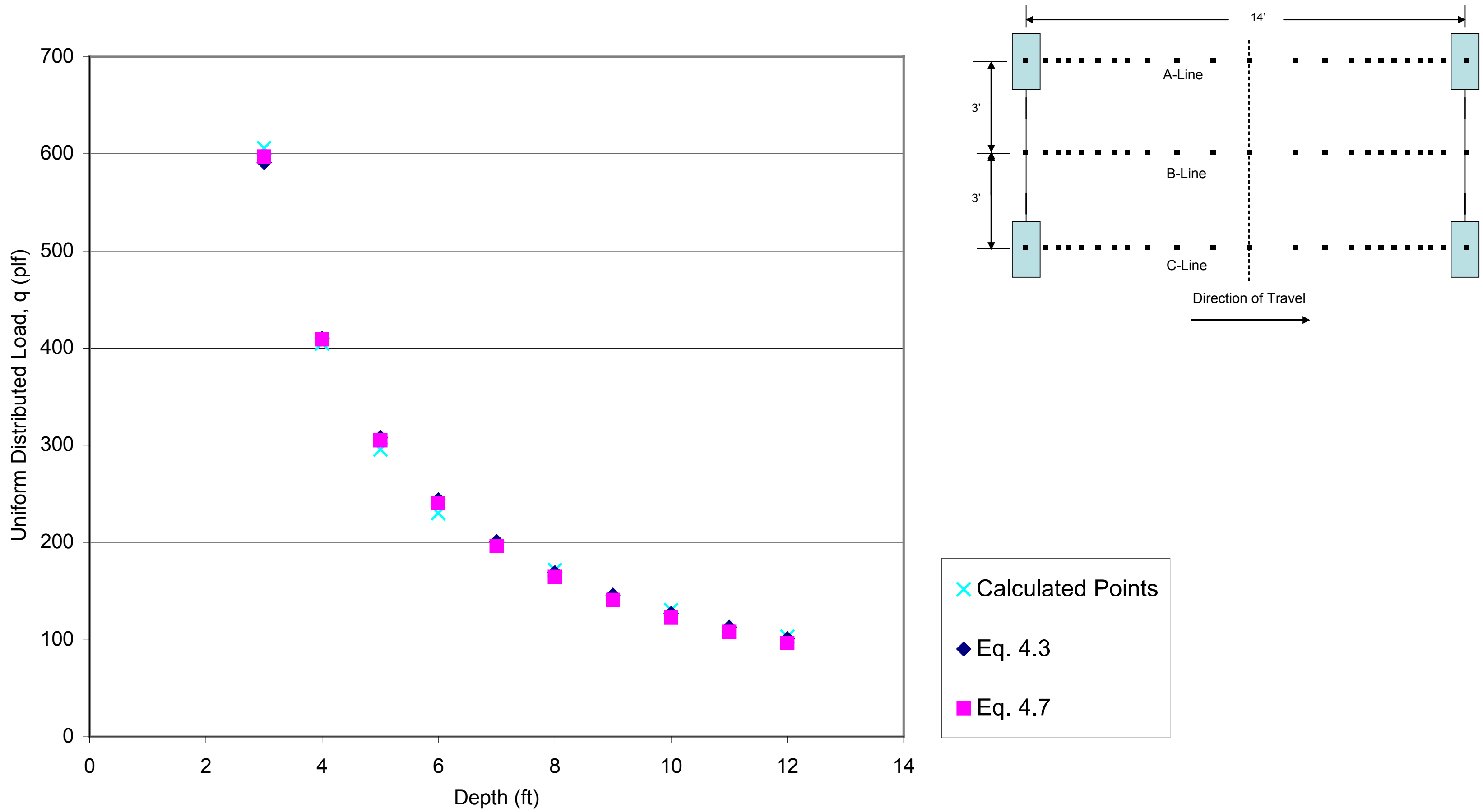

Figure 4-4. Best fit equation comparison – truck, 1 loaded lane

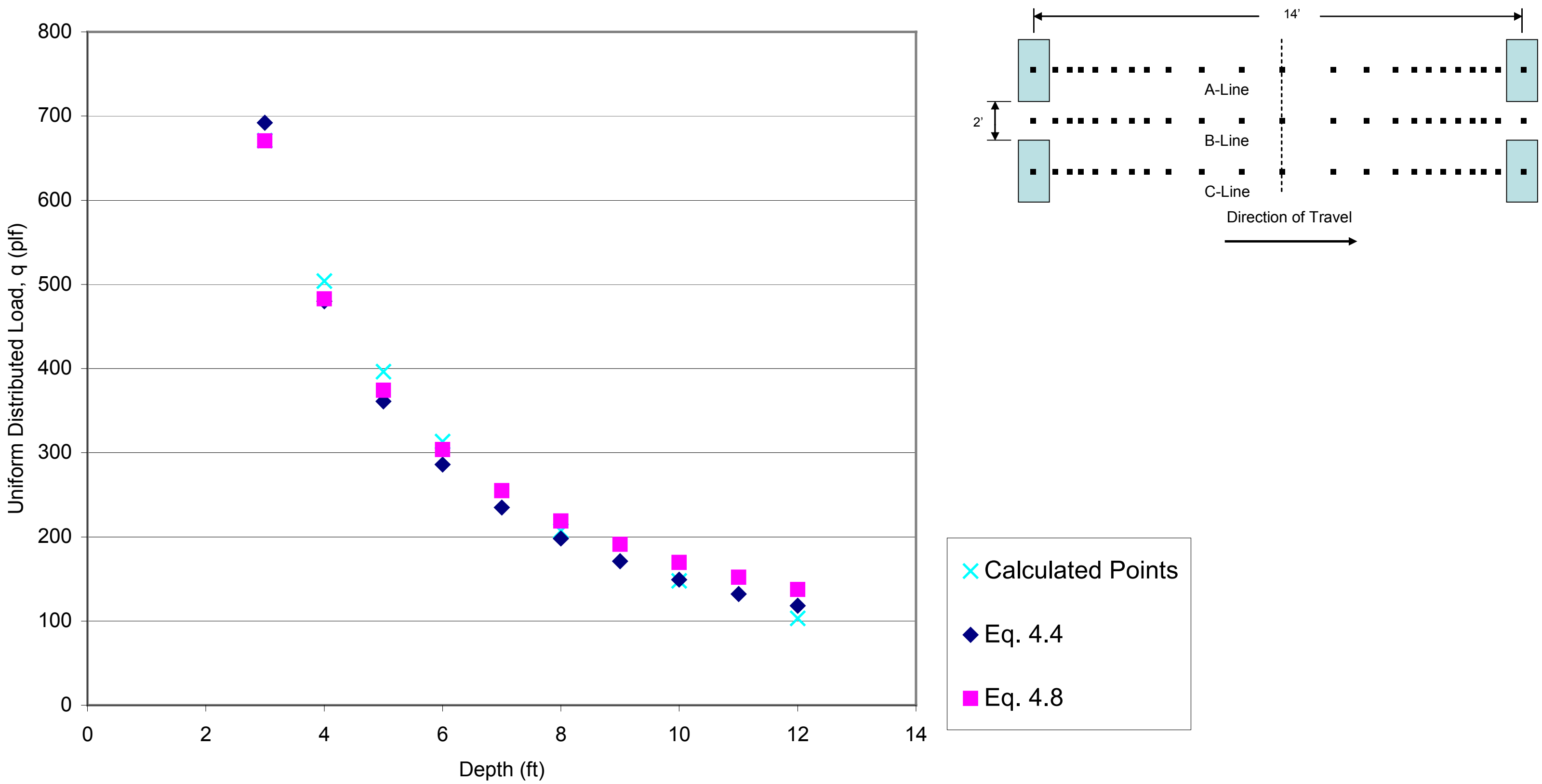

Figure 4-5. Best fit equation comparison – truck, 2 loaded lanes

4.2 Comparison of Results

Once a final design equation (Equation 4-9) was selected, it was important to compare the results it generated to ones that came as a result of using the AASHTO pressures previously calculated, as well as the results from the theoretical superposition method outlined in Chapter 3. Although the proposed design equation creates a uniform live load based on the depth of fill, moments were compared between the three methods (AASHTO, superposition or theoretical, and proposed). The proposed results are the ones generated by the proposed design equation. To get moments from the proposed equation, the formula of $M = ql^2/8$ was used to solve for the moment. Moments were compared because for the AASHTO method of live load distribution, the distributed load may not occupy the entire span length. This is different than the theoretical and proposed method, where the load occupies the entire span. Examples of AASHTO distributions are in Figure 4-5. To calculate the moments from the AASHTO pressures, the same method of moment calculation as described section 3.2.1 was used.

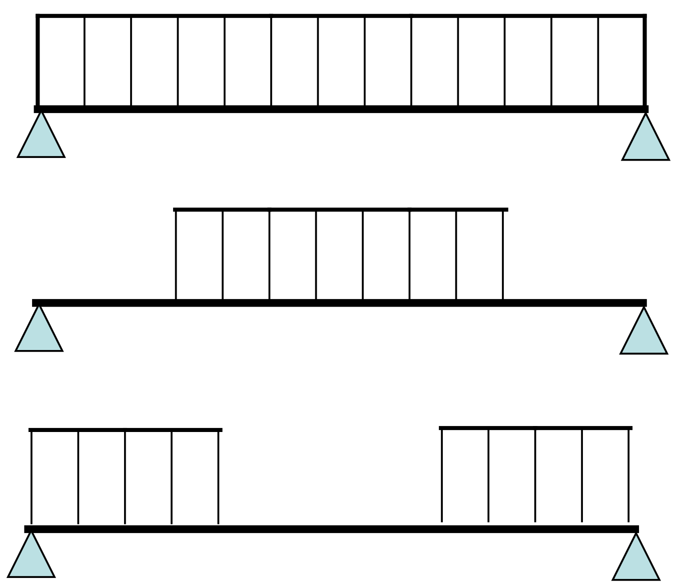

Figure 4-6. Possible AASHTO load distributions

For the moment comparisons, only the tandem, 2 loaded lane condition was used to calculate moments. This was decided because the final design equation, as well as the various methods of pressure calculation, produced the largest loads for this condition. However, the moments for different spans were calculated. Span lengths of 6 ft, 10 ft and 14 ft were used in the moment calculations. Table 4-2 shows the moments for the theoretical pressures, the AASHTO pressure, and the ones from the proposed design equation. Table 4-3 shows the moment results in ratio form. These ratios are plotted in Figures 4-7 to 4-9.

As can be seen in Tables 4-2 and 4-3, as well as in Figures 4-7 to 4-9, as the span length increased, the moments increased. This behavior was expected. The proposed moments matched closer to the theoretical and AASHTO moments at a span of 6 ft; the proposed moments deviated more from the theoretical and AASHTO ones as the span length increased. This was also expected because the proposed design equation was based on a 6 foot span length. The proposed moments were much larger than the theoretical and AASHTO moments at depths greater than 8ft. This is not a great concern because the AASHTO specification states that the live load may be neglected where the depth of fill is more than 8 ft and exceeds the span length. The proposed moments were closer to the theoretical moments at depths of 6 ft or less, and closer to the AASHTO moments at depths greater than 8 ft. The AASHTO moments were lower than the theoretical moments at depths less than 8 ft, but were larger than the theoretical moments at depths greater than 8 ft. Based on the coefficient of variance (CV), the proposed moments matched closer to the AASHTO moments than to the theoretical moments. This is acceptable because the AASHTO moments are close to what are currently being used for design.

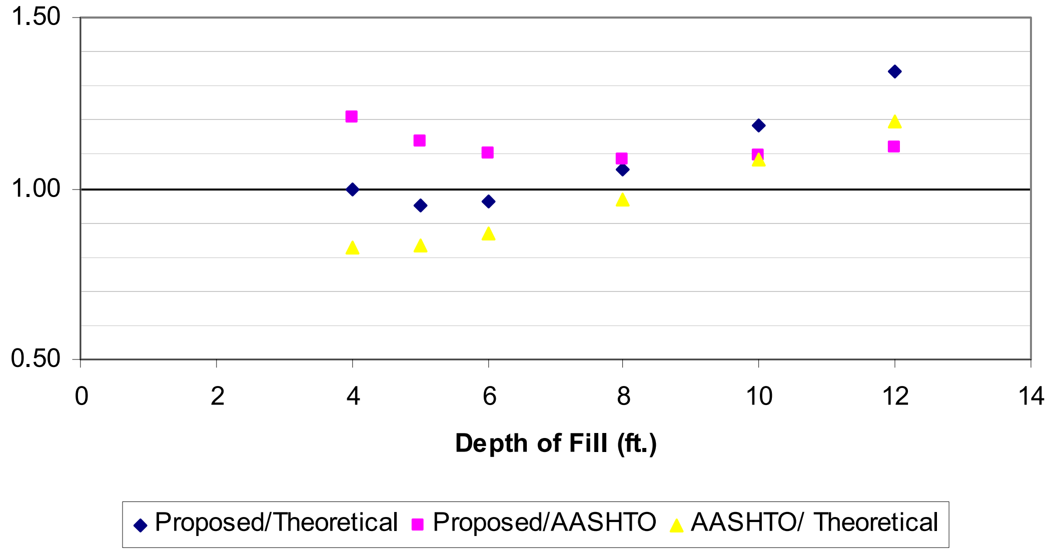

Figure 4-7. Moment ratio comparison – 6 foot span length

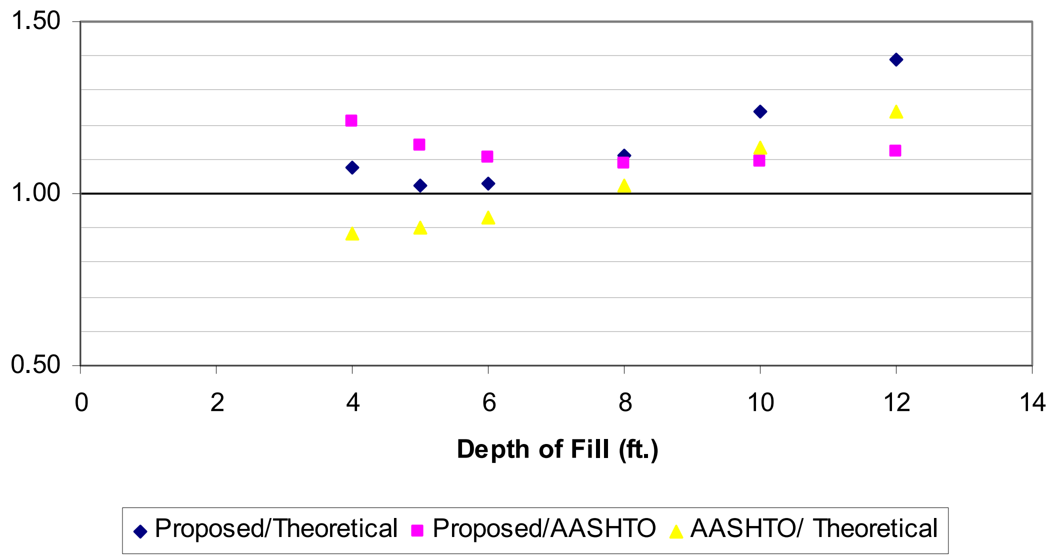

Figure 4-8. Moment ratio comparison – 10 foot span length

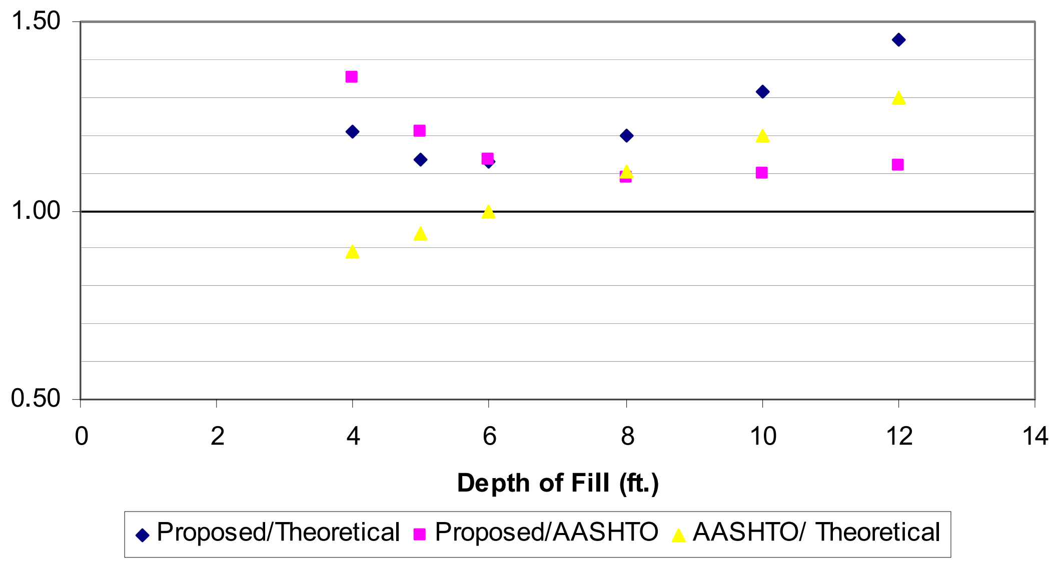

Figure 4-9. Moment ratio comparison – 14 foot span length

Table 4-2. Moment comparison

Span = 6'								
Moment (lb-ft)	Depth of Fill (ft)							
	2	3	4	5	6	8	10	12
Theoretical	4032	3049	2596	2177	1795	1229	872	643
AASHTO	3977	3186	2142	1818	1562	1193	945	770
Proposed	5175	3450	2588	2070	1725	1294	1035	863
Span = 10'								
Moment (lb-ft)	Depth of Fill (ft)							
	2	3	4	5	6	8	10	12
Theoretical	10939	7975	6699	5621	4658	3232	2320	1727
AASHTO	11351	8588	5930	5050	4338	3313	2625	2138
Proposed	14375	9583	7188	5750	4792	3594	2875	2396
Span = 14'								
Moment (lb-ft)	Depth of Fill (ft)							
	2	3	4	5	6	8	10	12
Theoretical	18478	13669	11663	9908	8307	5881	4289	3230
AASHTO	18917	14452	10420	9308	8278	6493	5145	4190
Proposed	28175	18783	14088	11270	9392	7044	5635	4696

Table 4-3. Moment ratios

Span = 6'									
	Depth of fill (ft)								Coefficient
Moment (lb-ft)	2	3	4	5	6	8	10	12	of variance
$M_{Proposed}/M_{Theoretical}$	1.29	1.12	0.97	0.92	0.92	0.99	1.10	1.24	14%
$M_{AASHTO}/ M_{Theoretical}$	0.99	1.04	0.83	0.84	0.87	0.97	1.08	1.20	16%
$M_{Proposed}/M_{AASHTO}$	1.31	1.07	1.18	1.10	1.05	1.02	1.02	1.03	4%
Span = 10'									
	Depth of fill (ft)								Coefficient
Moment (lb-ft)	2	3	4	5	6	8	10	12	of variance
$M_{Proposed}/M_{Theoretical}$	1.32	1.19	1.04	0.98	0.98	1.05	1.15	1.28	13%
$M_{AASHTO}/ M_{Theoretical}$	1.04	1.08	0.89	0.90	0.93	1.03	1.13	1.24	14%
$M_{Proposed}/M_{AASHTO}$	1.28	1.10	1.18	1.10	1.05	1.02	1.02	1.03	4%
Span = 14'									
	Depth of fill (ft)								Coefficient
Moment (lb-ft)	2	3	4	5	6	8	10	12	of variance
$M_{Proposed}/M_{Theoretical}$	1.54	1.36	1.18	1.10	1.08	1.13	1.22	1.34	10%
$M_{AASHTO}/ M_{Theoretical}$	1.02	1.06	0.89	0.94	1.00	1.10	1.20	1.30	15%
$M_{Proposed}/M_{AASHTO}$	1.50	1.28	1.32	1.17	1.08	1.02	1.02	1.03	9%

CHAPTER 5
CONCLUSIONS AND RECOMENDATIONS

This chapter summarizes the work completed for this project and offers suggestions for further research that may refine the results presented here.

5.1 Conclusions

The final goal for this project was to develop a design equation that could predict design live loads to be used in place of the current AASHTO recommended method. First, the superposition method of stress calculation was used to develop a stress distribution on a culvert for various depths of fill and various load scenarios. The load scenarios tested corresponded to the AASHTO tandem and truck geometries, placed either in a one or two loaded lane configuration. Based on the four distributions generated (one for each load condition), shears and moments acting on the top slab of the box culvert were calculated. The moments calculated were then used to back calculate a uniform distributed load that would generate the same maximum moment in the culvert. These uniformly distributed loads were then plotted against the depth of fill and an equation was found that reasonably fit the data. This equation is recommended as the final live load design equation.

The superposition method of stress calculations provided viable results without making too many assumptions that drastically violated real-life conditions. It was found that in most cases studied in this report, that the maximum moment controlled design. To develop the live load design equation, the span of the culvert was not included as an input. The equivalent uniformly distributed loads, for the most part, varied very little with the span of the culvert. Therefore the peak equivalent uniformly distributed load was used. This was for a 6 foot span, with the tandem 2 loaded lane condition. This created a conservative design equation. The final recommended equation is a simplified version of Equation 4-2, and is shown here again as Equation 5-1. The equivalent uniformly distributed load is q, with units of plf, and the depth of fill is z with units in feet.

$$q = \frac{2300}{z} \tag{5-1}$$

5.2 Recommendations for Further Research

First, it is recommended that this equation be only used for culverts with the span lengths that were in the range tested here; 6 foot to 14 foot spans. For span lengths less than 6 ft, the design equation may produce moments that are lower than anticipated ones. For span lengths greater than 14 ft, the design equation may produce moments that are increasingly conservative as the span length increases. If span lengths outside of the range studied here are to be used, the designer should use care when applying Equation 5-1. Also, Equation 5-1 should not be used for depths of fill 2ft and less. In those circumstances, the effect of the fill to dissipate the live load should be neglected, as stated in the AASHTO specification.

The primary suggestion for further work is to field test a full size box culvert, or an analytical model. As described in Chapter 2, field loadings of culverts have been completed in the past, however setting up a load test under similar conditions as the ones used in this project would aid in comparing the theoretical results presented here with field data. A comparison with recent field data would be the best approach to validate the stress distributions presented here.

Further refinement could be achieved by more rigorous statistical analysis of the best-fit equations presented here. Also, finite element analysis could prove to be beneficial because of its ability to model soil conditions more accurately. The methods used here were hardly exhaustive. The final results presented here are believed to produce live loads that are fit to be implemented, however further analysis could be completed to refine them.

These areas of further research are important in order to confirm the validity of the final design equation presented here.

APPENDIX A
STRESS CACLULATIONS

Table A-1. Sample Boussinesq stress calculation, tandem, 1 loaded lane

z = 2'

Grid	Wheel 1				Wheel 2				Wheel 3				Wheel 4				Total Δq
Point	z (ft)	r (ft)	P (kips)	q (psf)	z (ft)	r (ft)	P (kips)	q (psf)	z (ft)	r (ft)	P (kips)	q (psf)	z (ft)	r (ft)	P (kips)	q (psf)	(psf)
A	2	0	12.5	1492.08	2	4	12.5	26.69	2	6	12.5	4.72	2	7.211	12.5	2.03	1525.52
B	2	2	12.5	263.76	2	2	12.5	263.76	2	6.32	12.5	3.73	2	6.32	12.5	3.73	534.99
C	2	4	12.5	26.69	2	0	12.5	1492.08	2	7.21	12.5	2.04	2	6	12.5	4.72	1525.52
D	2	6	12.5	4.72	2	2	12.5	263.76	2	8.48	12.5	0.95	2	6.32	12.5	3.73	273.16
E	2	8	12.5	1.25	2	4	12.5	26.69	2	10	12.5	0.43	2	7.21	12.5	2.04	30.41
F	2	10	12.5	0.43	2	6	12.5	4.72	2	11.66	12.5	0.21	2	8.48	12.5	0.95	6.31
G	2	12	12.5	0.18	2	8	12.5	1.25	2	13.41	12.5	0.10	2	10	12.5	0.43	1.97
H	2	3	12.5	78.36	2	5	12.5	10.54	2	3	12.5	78.36	2	5	12.5	10.54	177.80
I	2	3.6	12.5	40.31	2	3.6	12.5	40.31	2	3.6	12.5	40.31	2	3.6	12.5	40.31	161.23
J	2	5	12.5	10.54	2	3	12.5	78.36	2	5	12.5	10.54	2	3	12.5	78.36	177.80
K	2	6.71	12.5	2.84	2	3.6	12.5	40.31	2	6.71	12.5	2.84	2	3.6	12.5	40.31	86.29
L	2	8.54	12.5	0.92	2	5	12.5	10.54	2	8.54	12.5	0.92	2	5	12.5	10.54	22.92
M	2	10.44	12.5	0.35	2	6.708	12.5	2.84	2	10.44	12.5	0.35	2	6.708	12.5	2.84	6.39
N	2	12.37	12.5	0.15	2	8.54	12.5	0.92	2	12.37	12.5	0.15	2	8.54	12.5	0.92	2.15
O	2	6	12.5	4.72	2	7.211	12.5	2.03	2	0	12.5	1492.08	2	4	12.5	26.69	1525.52
P	2	6.32	12.5	3.73	2	6.32	12.5	3.73	2	2	12.5	263.76	2	2	12.5	263.76	534.99
Q	2	7.211	12.5	2.03	2	6	12.5	4.72	2	4	12.5	26.69	2	0	12.5	1492.08	1525.52
R	2	8.48	12.5	0.95	2	6.32	12.5	3.73	2	6	12.5	4.72	2	2	12.5	263.76	273.16
S	2	10	12.5	0.43	2	7.211	12.5	2.03	2	8	12.5	1.25	2	4	12.5	26.69	30.41
T	2	11.66	12.5	0.21	2	8.48	12.5	0.95	2	10	12.5	0.43	2	6	12.5	4.72	6.31
U	2	13.41	12.5	0.10	2	10	12.5	0.43	2	12	12.5	0.18	2	8	12.5	1.25	1.97

Design Tandem - One Loaded Lane

Boussinesq Method - 2 Feet of Fill

Max 1525.523

Solve for total increase in stress at discrete points by adding increase in stress from all four wheel loads

z = depth

r = horizontal distance from point load to where stress is desired

P = point load

Table A-2. Summary of Boussinesq stress calculations, tandem, 1 loaded lane

z = 2 ft			z = 3 ft			z = 4 ft			z = 5 ft		
Point	r (ft)	Stress (psf)	Point	r (ft)	Stress (psf)	Point	r (ft)	Stress (psf)	Point	r (ft)	Stress (psf)
U	10	2	U	10	6	U	10	11	U	10	18
T	8	6	T	8	17	T	8	29	T	8	40
S	6	30	S	6	62	S	6	85	S	6	98
R	4	273	R	4	289	R	4	255	R	4	220
Q	2	1526	Q	2	732	Q	2	469	Q	2	348
P	0	535	P	0	548	P	0	460	P	0	373
O	-2	1526	O	-2	732	O	-2	469	O	-2	348
R	-4	273	R	-4	289	R	-4	255	R	-4	220
S	-6	30	S	-6	62	S	-6	85	S	-6	98
T	-8	6	T	-8	17	T	-8	29	T	-8	40
U	-10	2	U	-10	6	U	-10	11	U	-10	18

z = 6 ft			z = 8 ft			z = 10 ft			z = 12 ft		
Point	r (ft)	Stress (psf)	Point	r (ft)	Stress (psf)	Point	r (ft)	Stress (psf)	Point	r (ft)	Stress (psf)
N	10	26	N	10	37	N	10	42	N	10	43
M	8	54	M	8	65	M	8	66	M	8	62
L	6	110	L	6	110	L	6	99	L	6	85
K	4	197	K	4	167	K	4	135	K	4	109
J	2	279	J	2	216	J	2	165	J	2	127
I	0	307	I	0	235	I	0	176	I	0	134
H	-2	279	H	-2	216	H	-2	165	H	-2	127
K	-4	197	K	-4	167	K	-4	135	K	-4	109
L	-6	110	L	-6	110	L	-6	99	L	-6	85
M	-8	54	M	-8	65	M	-8	66	M	-8	62
N	-10	26	N	-10	37	N	-10	42	N	-10	43

r = distance to centerline of wheel spacing

Critical line is one between the two wheels at depts greater than 5 ft

Table A-3. Sample superposition stress calculation, tandem, 1 loaded lane

z = 2'

Inputs	P	q_o	B	L
English (kips, ft, ksf)	12.500	9.018	1.666	0.832

Point A

	B'	L'	z (ft)	m	n	c	term 1	term 2	adj term 2	I	σ_z (psf)
I-1	0.833	0.416	2	0.417	0.208	1.217	0.284	0.157	0.157	0.035	1266.4

Point B

	B'	L'	z (ft)	m	n	c	term 1	term 2	adj term 2	I	σ_z (psf)
I-1	0.833	2.416	2	0.417	1.208	2.633	0.781	0.601	0.601	0.110	256.716
I-2	0.833	1.584	2	0.417	0.792	1.801	0.721	0.482	0.482	0.096	
I-3	0.833	2.416	2	0.417	1.208	2.633	0.781	0.601	0.601	0.110	
I-4	0.833	1.584	2	0.417	0.792	1.801	0.721	0.482	0.482	0.096	

Point C

	B'	L'	z (ft)	m	n	c	term 1	term 2	adj term 2	I	σ_z (psf)
I-1	0.833	4.416	2	0.417	2.208	6.049	0.765	0.716	0.716	0.118	26.7987
I-2	0.833	3.584	2	0.417	1.792	4.385	0.777	0.685	0.685	0.116	
I-3	0.833	4.416	2	0.417	2.208	6.049	0.765	0.716	0.716	0.118	
I-4	0.833	3.584	2	0.417	1.792	4.385	0.777	0.685	0.685	0.116	

Point D

	B'	L'	z (ft)	m	n	c	term 1	term 2	adj term 2	I	σ_z (psf)
I-1	0.833	6.416	2	0.417	3.208	11.465	0.742	0.752	0.752	0.119	4.74002
I-2	0.833	5.584	2	0.417	2.792	8.969	0.750	0.741	0.741	0.119	
I-3	0.833	6.416	2	0.417	3.208	11.465	0.742	0.752	0.752	0.119	
I-4	0.833	5.584	2	0.417	2.792	8.969	0.750	0.741	0.741	0.119	

Point E

	B'	L'	z (ft)	m	n	c	term 1	term 2	adj term 2	I	σ_z (psf)
I-1	0.833	8.416	2	0.417	4.208	18.881	0.731	0.767	0.767	0.119	1.25635
I-2	0.833	7.584	2	0.417	3.792	15.553	0.735	0.762	0.762	0.119	
I-3	0.833	8.416	2	0.417	4.208	18.881	0.731	0.767	0.767	0.119	
I-4	0.833	7.584	2	0.417	3.792	15.553	0.735	0.762	0.762	0.119	

Point F

	B'	L'	z (ft)	m	n	c	term 1	term 2	adj term 2	I	σ_z (psf)
I-1	0.833	10.416	2	0.417	5.208	28.297	0.724	0.774	0.774	0.119	0.4339
I-2	0.833	9.584	2	0.417	4.792	24.137	0.726	0.772	0.772	0.119	
I-3	0.833	10.416	2	0.417	5.208	28.297	0.724	0.774	0.774	0.119	
I-4	0.833	9.584	2	0.417	4.792	24.137	0.726	0.772	0.772	0.119	

Point G

	B'	L'	z (ft)	m	n	c	term 1	term 2	adj term 2	I	σ_z (psf)
I-1	0.833	12.416	2	0.417	6.208	39.713	0.720	0.779	0.779	0.119	0.17949
I-2	0.833	11.584	2	0.417	5.792	34.721	0.721	0.777	0.777	0.119	
I-3	0.833	12.416	2	0.417	6.208	39.713	0.720	0.779	0.779	0.119	
I-4	0.833	11.584	2	0.417	5.792	34.721	0.721	0.777	0.777	0.119	

Point H

	B'	L'	z (ft)	m	n	c	term 1	term 2	adj term 2	I	σ_z (psf)
I-1	3.833	0.416	2	1.917	0.208	4.716	0.430	0.363	0.363	0.063	91.4519
I-2	2.167	0.416	2	1.084	0.208	2.217	0.429	0.300	0.300	0.058	
I-3	3.833	0.416	2	1.917	0.208	4.716	0.430	0.363	0.363	0.063	
I-4	2.167	0.416	2	1.084	0.208	2.217	0.429	0.300	0.300	0.058	

Table A-3. Continued

Point I

	B'	L'	z (ft)	m	n	c	term 1	term 2	adj term 2	I	σ_z (psf)
I-1	3.833	2.416	2	1.917	1.208	6.132	1.160	1.504	1.504	0.212	44.1215
I-2	3.833	1.584	2	1.917	0.792	5.300	1.093	1.166	1.166	0.180	
I-3	2.167	2.416	2	1.084	1.208	3.633	1.190	1.203	1.203	0.190	
I-4	2.167	1.584	2	1.084	0.792	2.801	1.102	0.948	0.948	0.163	

Point J

	B'	L'	z (ft)	m	n	c	term 1	term 2	adj term 2	I	σ_z (psf)
I-1	3.833	4.416	2	1.917	2.208	9.548	1.052	-1.261	1.880	0.233	10.9469
I-2	3.833	3.584	2	1.917	1.792	7.884	1.104	-1.371	1.771	0.229	
I-3	2.167	4.416	2	1.084	2.208	7.049	1.136	1.467	1.467	0.207	
I-4	2.167	3.584	2	1.084	1.792	5.385	1.167	1.393	1.393	0.204	

Point K

	B'	L'	z (ft)	m	n	c	term 1	term 2	adj term 2	I	σ_z (psf)
I-1	3.833	6.416	2	1.917	3.208	14.964	0.962	-1.123	2.018	0.237	2.8855
I-2	3.833	5.584	2	1.917	2.792	12.468	0.993	-1.167	1.975	0.236	
I-3	2.167	6.416	2	1.084	3.208	12.465	1.080	1.555	1.555	0.210	
I-4	2.167	5.584	2	1.084	2.792	9.969	1.099	1.528	1.528	0.209	

Point L

	B'	L'	z (ft)	m	n	c	term 1	term 2	adj term 2	I	σ_z (psf)
I-1	3.833	8.416	2	1.917	4.208	22.380	0.912	-1.061	2.081	0.238	0.92479
I-2	3.833	7.584	2	1.917	3.792	19.052	0.929	-1.082	2.060	0.238	
I-3	2.167	8.416	2	1.084	4.208	19.881	1.050	-1.549	1.593	0.210	
I-4	2.167	7.584	2	1.084	3.792	16.553	1.060	-1.561	1.581	0.210	

Point M

	B'	L'	z (ft)	m	n	c	term 1	term 2	adj term 2	I	σ_z (psf)
I-1	3.833	10.416	2	1.917	5.208	31.796	0.883	-1.028	2.113	0.238	0.3533
I-2	3.833	9.584	2	1.917	4.792	27.636	0.893	-1.040	2.102	0.238	
I-3	2.167	10.416	2	1.084	5.208	29.297	1.033	-1.529	1.612	0.211	
I-4	2.167	9.584	2	1.084	4.792	25.137	1.039	-1.536	1.606	0.210	

Point N

	B'	L'	z (ft)	m	n	c	term 1	term 2	adj term 2	I	σ_z (psf)
I-1	3.833	12.416	2	1.917	6.208	43.212	0.866	-1.010	2.132	0.239	0.15502
I-2	3.833	11.584	2	1.917	5.792	38.220	0.872	-1.016	2.125	0.239	
I-3	2.167	12.416	2	1.084	6.208	40.713	1.023	-1.518	1.624	0.211	
I-4	2.167	11.584	2	1.084	5.792	35.721	1.027	-1.522	1.620	0.211	

Point O

	B'	L'	z (ft)	m	n	c	term 1	term 2	adj term 2	I	σ_z (psf)
I-1	6.833	0.416	2	3.417	0.208	12.716	0.413	0.393	0.393	0.064	5.07507
I-2	5.167	0.416	2	2.584	0.208	7.718	0.421	0.382	0.382	0.064	
I-3	6.833	0.416	2	3.417	0.208	12.716	0.413	0.393	0.393	0.064	
I-4	5.167	0.416	2	2.584	0.208	7.718	0.421	0.382	0.382	0.064	

Point P

	B'	L'	z (ft)	m	n	c	term 1	term 2	adj term 2	I	σ_z (psf)
I-1	6.833	2.416	2	3.417	1.208	14.132	1.066	-1.478	1.664	0.217	3.95149
I-2	6.833	1.584	2	3.417	0.792	13.300	1.029	1.277	1.277	0.183	
I-3	5.167	2.416	2	2.584	1.208	9.134	1.109	-1.539	1.603	0.216	
I-4	5.167	1.584	2	2.584	0.792	8.302	1.058	1.235	1.235	0.182	

Point Q

	B'	L'	z (ft)	m	n	c	term 1	term 2	adj term 2	I	σ_z (psf)
I-1	6.833	4.416	2	3.417	2.208	17.548	0.897	-1.014	2.128	0.241	2.115
I-2	6.833	3.584	2	3.417	1.792	15.884	0.972	-1.154	1.987	0.236	
I-3	5.167	4.416	2	2.584	2.208	12.550	0.968	-1.111	2.030	0.239	
I-4	5.167	3.584	2	2.584	1.792	10.886	1.032	-1.238	1.903	0.234	

Table A-3. Continued

Point R

	B'	L'	z (ft)	m	n	c	term 1	term 2	adj term 2	I	σ_z (psf)
I-1	6.833	6.416	2	3.417	3.208	22.964	0.766	-0.824	2.317	0.245	0.96937
I-2	6.833	5.584	2	3.417	2.792	20.468	0.812	-0.886	2.256	0.244	
I-3	5.167	6.416	2	2.584	3.208	17.966	0.856	-0.945	2.196	0.243	
I-4	5.167	5.584	2	2.584	2.792	15.470	0.895	-0.998	2.143	0.242	

Point S

	B'	L'	z (ft)	m	n	c	term 1	term 2	adj term 2	I	σ_z (psf)
I-1	6.833	8.416	2	3.417	4.208	30.380	0.691	-0.732	2.409	0.247	0.43832
I-2	6.833	7.584	2	3.417	3.792	27.052	0.717	-0.764	2.378	0.246	
I-3	5.167	8.416	2	2.584	4.208	25.382	0.793	-0.868	2.274	0.244	
I-4	5.167	7.584	2	2.584	3.792	22.054	0.815	-0.894	2.248	0.244	

Point T

	B'	L'	z (ft)	m	n	c	term 1	term 2	adj term 2	I	σ_z (psf)
I-1	6.833	10.416	2	3.417	5.208	39.796	0.646	-0.681	2.460	0.247	0.20742
I-2	6.833	9.584	2	3.417	4.792	35.636	0.662	-0.699	2.442	0.247	
I-3	5.167	10.416	2	2.584	5.208	34.798	0.757	-0.826	2.315	0.244	
I-4	5.167	9.584	2	2.584	4.792	30.638	0.770	-0.841	2.301	0.244	

Point U

	B'	L'	z (ft)	m	n	c	term 1	term 2	adj term 2	I	σ_z (psf)
I-1	6.833	12.416	2	3.417	6.208	51.212	0.618	-0.651	2.491	0.247	0.10445
I-2	6.833	11.584	2	3.417	5.792	46.220	0.628	-0.662	2.480	0.247	
I-3	5.167	12.416	2	2.584	6.208	46.214	0.734	-0.802	2.340	0.245	
I-4	5.167	11.584	2	2.584	5.792	41.222	0.742	-0.811	2.331	0.245	

Point AJ

	B'	L'	z (ft)	m	n	c	term 1	term 2	adj term 2	I	σ_z (psf)
I-1	0.833	0.917	2	0.417	0.459	1.384	0.545	0.322	0.322	0.069	1112.14
I-2	0.833	0.084	2	0.417	0.042	1.175	0.060	0.032	0.032	0.007	
I-3	0.833	0.917	2	0.417	0.459	1.384	0.545	0.322	0.322	0.069	
I-4	0.833	0.084	2	0.417	0.042	1.175	0.060	0.032	0.032	0.007	

Point AK

	B'	L'	z (ft)	m	n	c	term 1	term 2	adj term 2	I	σ_z (psf)
I-1	0.833	1.417	2	0.417	0.709	1.675	0.692	0.448	0.448	0.091	774.948
I-2	0.833	0.584	2	0.417	0.292	1.259	0.385	0.216	0.216	0.048	
I-3	0.833	1.417	2	0.417	0.709	1.675	0.692	0.448	0.448	0.091	
I-4	0.833	0.584	2	0.417	0.292	1.259	0.385	0.216	0.216	0.048	

Point AL

	B'	L'	z (ft)	m	n	c	term 1	term 2	adj term 2	I	σ_z (psf)
I-1	0.833	1.917	2	0.417	0.959	2.092	0.758	0.539	0.539	0.103	462.791
I-2	0.833	1.084	2	0.417	0.542	1.467	0.606	0.369	0.369	0.078	
I-3	0.833	1.917	2	0.417	0.959	2.092	0.758	0.539	0.539	0.103	
I-4	0.833	1.084	2	0.417	0.542	1.467	0.606	0.369	0.369	0.078	

Point AM

	B'	L'	z (ft)	m	n	c	term 1	term 2	adj term 2	I	σ_z (psf)
I-1	0.833	2.917	2	0.417	1.459	3.301	0.784	0.645	0.645	0.114	140.529
I-2	0.833	2.084	2	0.417	1.042	2.259	0.769	0.562	0.562	0.106	
I-3	0.833	2.917	2	0.417	1.459	3.301	0.784	0.645	0.645	0.114	
I-4	0.833	2.084	2	0.417	1.042	2.259	0.769	0.562	0.562	0.106	

Point AN

	B'	L'	z (ft)	m	n	c	term 1	term 2	adj term 2	I	σ_z (psf)
I-1	0.833	3.417	2	0.417	1.709	4.092	0.779	0.676	0.676	0.116	78.2438
I-2	0.833	2.584	2	0.417	1.292	2.843	0.783	0.618	0.618	0.111	
I-3	0.833	3.417	2	0.417	1.709	4.092	0.779	0.676	0.676	0.116	
I-4	0.833	2.584	2	0.417	1.292	2.843	0.783	0.618	0.618	0.111	

Table A-3. Continued

Point AO

	B'	L'	z (ft)	m	n	c	term 1	term 2	adj term 2	I	σ_z (psf)
I-1	0.833	3.917	2	0.417	1.959	5.009	0.772	0.699	0.699	0.117	44.9813
I-2	0.833	3.084	2	0.417	1.542	3.551	0.783	0.657	0.657	0.115	
I-3	0.833	3.917	2	0.417	1.959	5.009	0.772	0.699	0.699	0.117	
I-4	0.833	3.084	2	0.417	1.542	3.551	0.783	0.657	0.657	0.115	

Point AP

	B'	L'	z (ft)	m	n	c	term 1	term 2	adj term 2	I	σ_z (psf)
I-1	0.833	4.917	2	0.417	2.459	7.218	0.758	0.728	0.728	0.118	16.5804
I-2	0.833	4.084	2	0.417	2.042	5.343	0.769	0.705	0.705	0.117	
I-3	0.833	4.917	2	0.417	2.459	7.218	0.758	0.728	0.728	0.118	
I-4	0.833	4.084	2	0.417	2.042	5.343	0.769	0.705	0.705	0.117	

Point AQ

	B'	L'	z (ft)	m	n	c	term 1	term 2	adj term 2	I	σ_z (psf)
I-1	0.833	5.417	2	0.417	2.709	8.509	0.752	0.738	0.738	0.119	10.6039
I-2	0.833	4.584	2	0.417	2.292	6.427	0.762	0.720	0.720	0.118	
I-3	0.833	5.417	2	0.417	2.709	8.509	0.752	0.738	0.738	0.119	
I-4	0.833	4.584	2	0.417	2.292	6.427	0.762	0.720	0.720	0.118	

Point AR

	B'	L'	z (ft)	m	n	c	term 1	term 2	adj term 2	I	σ_z (psf)
I-1	0.833	5.917	2	0.417	2.959	9.926	0.747	0.746	0.746	0.119	6.99459
I-2	0.833	5.084	2	0.417	2.542	7.635	0.756	0.732	0.732	0.118	
I-3	0.833	5.917	2	0.417	2.959	9.926	0.747	0.746	0.746	0.119	
I-4	0.833	5.084	2	0.417	2.542	7.635	0.756	0.732	0.732	0.118	

Point AS

	B'	L'	z (ft)	m	n	c	term 1	term 2	adj term 2	I	σ_z (psf)
I-1	3.833	0.917	2	1.917	0.459	4.883	0.827	0.757	0.757	0.126	86.8534
I-2	3.833	0.084	2	1.917	0.042	4.675	0.090	0.074	0.074	0.013	
I-3	2.167	0.917	2	1.084	0.459	2.384	0.828	0.623	0.623	0.115	
I-4	2.167	0.084	2	1.084	0.042	2.176	0.090	0.062	0.062	0.012	

Point AT

	B'	L'	z (ft)	m	n	c	term 1	term 2	adj term 2	I	σ_z (psf)
I-1	3.833	1.417	2	1.917	0.709	5.175	1.050	1.076	1.076	0.169	74.6463
I-2	3.833	0.584	2	1.917	0.292	4.758	0.583	0.502	0.502	0.086	
I-3	2.167	1.417	2	1.084	0.709	2.676	1.057	0.878	0.878	0.154	
I-4	2.167	0.584	2	1.084	0.292	2.259	0.582	0.415	0.415	0.079	

Point AU

	B'	L'	z (ft)	m	n	c	term 1	term 2	adj term 2	I	σ_z (psf)
I-1	3.833	1.917	2	1.917	0.959	5.592	1.142	1.321	1.321	0.196	59.1401
I-2	3.833	1.084	2	1.917	0.542	4.967	0.920	0.872	0.872	0.143	
I-3	2.167	1.917	2	1.084	0.959	3.093	1.159	1.067	1.067	0.177	
I-4	2.167	1.084	2	1.084	0.542	2.468	0.922	0.715	0.715	0.130	

Point AV

	B'	L'	z (ft)	m	n	c	term 1	term 2	adj term 2	I	σ_z (psf)
I-1	3.833	2.917	2	1.917	1.459	6.800	1.144	-1.501	1.640	0.222	31.7543
I-2	3.833	2.084	2	1.917	1.042	5.759	1.154	1.388	1.388	0.202	
I-3	2.167	2.917	2	1.084	1.459	4.301	1.188	1.302	1.302	0.198	
I-4	2.167	2.084	2	1.084	1.042	3.260	1.175	1.118	1.118	0.182	

Point AW

	B'	L'	z (ft)	m	n	c	term 1	term 2	adj term 2	I	σ_z (psf)
I-1	3.833	3.417	2	1.917	1.709	7.592	1.115	-1.399	1.743	0.227	22.3749
I-2	3.833	2.584	2	1.917	1.292	6.342	1.158	1.554	1.554	0.216	
I-3	2.167	3.417	2	1.084	1.709	5.093	1.173	1.374	1.374	0.203	
I-4	2.167	2.584	2	1.084	1.292	3.843	1.192	1.240	1.240	0.194	

Table A-3. Continued

Point AX

	B'	L'	z (ft)	m	n	c	term 1	term 2	adj term 2	I	σ_z (psf)
I-1	3.833	3.917	2	1.917	1.959	8.509	1.083	-1.321	1.820	0.231	15.6483
I-2	3.833	3.084	2	1.917	1.542	7.051	1.135	-1.464	1.678	0.224	
I-3	2.167	3.917	2	1.084	1.959	6.010	1.154	1.427	1.427	0.205	
I-4	2.167	3.084	2	1.084	1.542	4.552	1.184	1.329	1.329	0.200	

Point AY

	B'	L'	z (ft)	m	n	c	term 1	term 2	adj term 2	I	σ_z (psf)
I-1	3.833	4.917	2	1.917	2.459	10.717	1.025	-1.214	1.927	0.235	7.72276
I-2	3.833	4.084	2	1.917	2.042	8.843	1.072	-1.300	1.842	0.232	
I-3	2.167	4.917	2	1.084	2.459	8.218	1.119	1.497	1.497	0.208	
I-4	2.167	4.084	2	1.084	2.042	6.344	1.148	1.442	1.442	0.206	

Point AZ

	B'	L'	z (ft)	m	n	c	term 1	term 2	adj term 2	I	σ_z (psf)
I-1	3.833	5.417	2	1.917	2.709	12.009	1.000	-1.177	1.964	0.236	5.4977
I-2	3.833	4.584	2	1.917	2.292	9.926	1.043	-1.244	1.897	0.234	
I-3	2.167	5.417	2	1.084	2.709	9.510	1.104	1.521	1.521	0.209	
I-4	2.167	4.584	2	1.084	2.292	7.427	1.130	1.478	1.478	0.208	

Point BA

	B'	L'	z (ft)	m	n	c	term 1	term 2	adj term 2	I	σ_z (psf)
I-1	3.833	5.917	2	1.917	2.959	13.426	0.980	-1.147	1.994	0.237	3.95985
I-2	3.833	5.084	2	1.917	2.542	11.135	1.016	-1.201	1.940	0.235	
I-3	2.167	5.917	2	1.084	2.959	10.927	1.091	1.540	1.540	0.209	
I-4	2.167	5.084	2	1.084	2.542	8.636	1.113	1.506	1.506	0.208	

Point BB

	B'	L'	z (ft)	m	n	c	term 1	term 2	adj term 2	I	σ_z (psf)
I-1	6.833	0.917	2	3.417	0.459	12.883	0.790	0.823	0.823	0.128	4.99818
I-2	6.833	0.084	2	3.417	0.042	12.674	0.087	0.081	0.081	0.013	
I-3	5.167	0.917	2	2.584	0.459	7.885	0.807	0.798	0.798	0.128	
I-4	5.167	0.084	2	2.584	0.042	7.676	0.088	0.078	0.078	0.013	

Point BC

	B'	L'	z (ft)	m	n	c	term 1	term 2	adj term 2	I	σ_z (psf)
I-1	6.833	1.417	2	3.417	0.709	13.174	0.993	1.176	1.176	0.173	4.76085
I-2	6.833	0.584	2	3.417	0.292	12.758	0.559	0.545	0.545	0.088	
I-3	5.167	1.417	2	2.584	0.709	8.176	1.019	1.139	1.139	0.172	
I-4	5.167	0.584	2	2.584	0.292	7.760	0.570	0.529	0.529	0.087	

Point BD

	B'	L'	z (ft)	m	n	c	term 1	term 2	adj term 2	I	σ_z (psf)
I-1	6.833	1.917	2	3.417	0.959	13.591	1.066	1.453	1.453	0.200	4.39951
I-2	6.833	1.084	2	3.417	0.542	12.966	0.876	0.950	0.950	0.145	
I-3	5.167	1.917	2	2.584	0.959	8.593	1.101	1.403	1.403	0.199	
I-4	5.167	1.084	2	2.584	0.542	7.968	0.896	0.921	0.921	0.145	

Point BE

	B'	L'	z (ft)	m	n	c	term 1	term 2	adj term 2	I	σ_z (psf)
I-1	6.833	2.917	2	3.417	1.459	14.800	1.033	-1.315	1.827	0.228	3.47302
I-2	6.833	2.084	2	3.417	1.042	13.758	1.072	1.530	1.530	0.207	
I-3	5.167	2.917	2	2.584	1.459	9.802	1.083	-1.387	1.755	0.226	
I-4	5.167	2.084	2	2.584	1.042	8.760	1.109	1.476	1.476	0.206	

Point BF

	B'	L'	z (ft)	m	n	c	term 1	term 2	adj term 2	I	σ_z (psf)
I-1	6.833	3.417	2	3.417	1.709	15.591	0.988	-1.190	1.952	0.234	2.98894
I-2	6.833	2.584	2	3.417	1.292	14.342	1.057	-1.418	1.723	0.221	
I-3	5.167	3.417	2	2.584	1.709	10.593	1.046	-1.271	1.871	0.232	
I-4	5.167	2.584	2	2.584	1.292	9.344	1.103	-1.483	1.659	0.220	

Table A-3. Continued

Point BG

	B'	L'	z (ft)	m	n	c	term 1	term 2	adj term 2	I	σ_z (psf)
I-1	6.833	3.917	2	3.417	1.959	16.508	0.941	-1.091	2.050	0.238	2.53127
I-2	6.833	3.084	2	3.417	1.542	15.050	1.018	-1.269	1.872	0.230	
I-3	5.167	3.917	2	2.584	1.959	11.510	1.005	-1.181	1.960	0.236	
I-4	5.167	3.084	2	2.584	1.542	10.052	1.071	-1.344	1.797	0.228	

Point BH

	B'	L'	z (ft)	m	n	c	term 1	term 2	adj term 2	I	σ_z (psf)
I-1	6.833	4.917	2	3.417	2.459	18.717	0.858	-0.951	2.190	0.243	1.75464
I-2	6.833	4.084	2	3.417	2.042	16.842	0.926	-1.063	2.078	0.239	
I-3	5.167	4.917	2	2.584	2.459	13.719	0.934	-1.056	2.086	0.240	
I-4	5.167	4.084	2	2.584	2.042	11.844	0.992	-1.156	1.986	0.237	

Point BI

	B'	L'	z (ft)	m	n	c	term 1	term 2	adj term 2	I	σ_z (psf)
I-1	6.833	5.417	2	3.417	2.709	20.008	0.823	-0.901	2.241	0.244	1.445
I-2	6.833	4.584	2	3.417	2.292	17.926	0.883	-0.991	2.150	0.241	
I-3	5.167	5.417	2	2.584	2.709	15.010	0.904	-1.011	2.130	0.241	
I-4	5.167	4.584	2	2.584	2.292	12.928	0.956	-1.091	2.050	0.239	

Point BJ

	B'	L'	z (ft)	m	n	c	term 1	term 2	adj term 2	I	σ_z (psf)
I-1	6.833	5.917	2	3.417	2.959	21.425	0.792	-0.859	2.283	0.245	1.18531
I-2	6.833	5.084	2	3.417	2.542	19.134	0.846	-0.933	2.208	0.243	
I-3	5.167	5.917	2	2.584	2.959	16.427	0.878	-0.975	2.166	0.242	
I-4	5.167	5.084	2	2.584	2.542	14.136	0.923	-1.040	2.102	0.241	

Point CC

	B'	L'	z (ft)	m	n	c	term 1	term 2	adj term 2	I	σ_z (psf)
I-1	0.833	7.416	2	0.417	3.708	14.923	0.736	0.761	0.761	0.119	2.34402
I-2	0.833	6.584	2	0.417	3.292	12.011	0.741	0.753	0.753	0.119	
I-3	0.833	7.416	2	0.417	3.708	14.923	0.736	0.761	0.761	0.119	
I-4	0.833	6.584	2	0.417	3.292	12.011	0.741	0.753	0.753	0.119	

Point CD

	B'	L'	z (ft)	m	n	c	term 1	term 2	adj term 2	I	σ_z (psf)
I-1	3.833	7.416	2	1.917	3.708	18.422	0.933	-1.087	2.055	0.238	1.59445
I-2	3.833	6.584	2	1.917	3.292	15.510	0.956	-1.116	2.026	0.237	
I-3	2.167	7.416	2	1.084	3.708	15.923	1.063	-1.564	1.578	0.210	
I-4	2.167	6.584	2	1.084	3.292	13.011	1.077	1.560	1.560	0.210	

Point CE

	B'	L'	z (ft)	m	n	c	term 1	term 2	adj term 2	I	σ_z (psf)
I-1	6.833	7.416	2	3.417	3.708	26.422	0.723	-0.771	2.371	0.246	0.64962
I-2	6.833	6.584	2	3.417	3.292	23.510	0.758	-0.814	2.328	0.246	
I-3	5.167	7.416	2	2.584	3.708	21.424	0.820	-0.900	2.241	0.244	
I-4	5.167	6.584	2	2.584	3.292	18.512	0.849	-0.937	2.205	0.243	

Point CH

	B'	L'	z (ft)	m	n	c	term 1	term 2	adj term 2	I	σ_z (psf)
I-1	0.833	9.416	2	0.417	4.708	23.339	0.727	0.771	0.771	0.119	0.7188
I-2	0.833	8.584	2	0.417	4.292	19.595	0.730	0.768	0.768	0.119	
I-3	0.833	9.416	2	0.417	4.708	23.339	0.727	0.771	0.771	0.119	
I-4	0.833	8.584	2	0.417	4.292	19.595	0.730	0.768	0.768	0.119	

Point CI

	B'	L'	z (ft)	m	n	c	term 1	term 2	adj term 2	I	σ_z (psf)
I-1	3.833	9.416	2	1.917	4.708	26.838	0.896	-1.042	2.099	0.238	0.56052
I-2	3.833	8.584	2	1.917	4.292	23.094	0.909	-1.057	2.084	0.238	
I-3	2.167	9.416	2	1.084	4.708	24.339	1.041	-1.537	1.604	0.210	
I-4	2.167	8.584	2	1.084	4.292	20.595	1.048	-1.546	1.595	0.210	

Point CJ

	B'	L'	z (ft)	m	n	c	term 1	term 2	adj term 2	I	σ_z (psf)
I-1	6.833	9.416	2	3.417	4.708	34.838	0.665	-0.703	2.438	0.247	0.29932
I-2	6.833	8.584	2	3.417	4.292	31.094	0.686	-0.727	2.415	0.247	
I-3	5.167	9.416	2	2.584	4.708	29.840	0.773	-0.844	2.297	0.244	
I-4	5.167	8.584	2	2.584	4.292	26.096	0.789	-0.863	2.278	0.244	

Design Tandem - Single Loaded Lane
Superposition Method
Single Wheel Loading - Pont A being the reference point
This spreadsheet calculates the stress at a given point point based on a single wheel load located at point A
Note: Calculations for other depths and load conditions are similar
m = B'/z   n = L'/z   B', L' = length and width of the uniformly loaded area

Table A-4. Sample superposition total stress calculation

z = 2'

Point	Wheel 1		Wheel 2		Wheel 3		Wheel 4		Total
	Point	Stress	Point	Stress	Point	Stress	Point	Stress	Stress
A	A	1266.40	C	26.80	O	5.08	Q	2.11	1300.39
B	B	256.72	B	256.72	P	3.95	P	3.95	521.33
C	C	26.80	A	1266.40	Q	2.11	O	5.08	1300.39
D	D	4.74	B	256.72	R	0.97	P	3.95	266.38
E	E	1.26	C	26.80	S	0.44	Q	2.11	30.61
F	F	0.43	D	4.74	T	0.21	R	0.97	6.35
G	G	0.18	E	1.26	U	0.10	S	0.44	1.98
H	H	91.45	J	10.95	H	91.45	J	10.95	204.80
I	I	44.12	I	44.12	I	44.12	I	44.12	176.49
J	J	10.95	H	91.45	J	10.95	H	91.45	204.80
K	K	2.89	I	44.12	K	2.89	I	44.12	94.01
L	L	0.92	J	10.95	L	0.92	J	10.95	23.74
M	M	0.35	K	2.89	M	0.35	K	2.89	6.48
N	N	0.16	L	0.92	N	0.16	L	0.92	2.16
O	O	5.08	Q	2.11	A	1266.40	C	26.80	1300.39
P	P	3.95	P	3.95	B	256.72	B	256.72	521.33
Q	Q	2.11	O	5.08	C	26.80	A	1266.40	1300.39
R	R	0.97	P	3.95	D	4.74	B	256.72	266.38
S	S	0.44	Q	2.11	E	1.26	C	26.80	30.61
T	T	0.21	R	0.97	F	0.43	D	4.74	6.35
U	U	0.10	S	0.44	G	0.18	E	1.26	1.98
AJ	AJ	1112.14	AO	44.98	BB	5.00	BG	2.53	1164.65
AK	AK	774.95	AN	78.24	BC	4.76	BF	2.99	860.94
AL	AL	462.79	AM	140.53	BD	4.40	BE	3.47	611.19
AM	AM	140.53	AL	462.79	BE	3.47	BD	4.40	611.19
AN	AN	78.24	AK	774.95	BF	2.99	BC	4.76	860.94
AO	AO	44.98	AJ	1112.14	BG	2.53	BB	5.00	1164.65
AP	AP	16.58	AJ	1112.14	BH	1.75	BB	5.00	1135.47
AQ	AQ	10.60	AK	774.95	BI	1.45	BC	4.76	791.76
AR	AR	6.99	AL	462.79	BJ	1.19	BD	4.40	475.37
AS	AS	86.85	AX	15.65	AS	86.85	AX	15.65	205.00
AT	AT	74.65	AW	22.37	AT	74.65	AW	22.37	194.04
AU	AU	59.14	AV	31.75	AU	59.14	AV	31.75	181.79
AV	AV	31.75	AU	59.14	AV	31.75	AU	59.14	181.79
AW	AW	22.37	AT	74.65	AW	22.37	AT	74.65	194.04
AX	AX	15.65	AS	86.85	AX	15.65	AS	86.85	205.00
AY	AY	7.72	AS	86.85	AY	7.72	AS	86.85	189.15
AZ	AZ	5.50	AT	74.65	AZ	5.50	AT	74.65	160.29
BA	BA	3.96	AU	59.14	BA	3.96	AU	59.14	126.20
BB	BB	5.00	BG	2.53	AJ	1112.14	AO	44.98	1164.65
BC	BC	4.76	BF	2.99	AK	774.95	AN	78.24	860.94
BD	BD	4.40	BE	3.47	AL	462.79	AM	140.53	611.19
BE	BE	3.47	BD	4.40	AM	140.53	AL	462.79	611.19
BF	BF	2.99	BC	4.76	AN	78.24	AK	774.95	860.94
BG	BG	2.53	BB	5.00	AO	44.98	AJ	1112.14	1164.65
BH	BH	1.75	BB	5.00	AP	16.58	AJ	1112.14	1135.47
BI	BI	1.45	BC	4.76	AQ	10.60	AK	774.95	791.76
BJ	BJ	1.19	BD	4.40	AR	6.99	AL	462.79	475.37
CC	CC	2.34	AN	78.24	CE	0.65	BF	2.99	84.23
CD	CD	1.59	AW	22.37	CD	1.59	AW	22.37	47.94
CE	CE	0.65	BF	2.99	CC	2.34	AN	78.24	84.23
CH	CH	0.72	AQ	10.60	CJ	0.30	BI	1.45	13.07
CI	CI	0.56	AZ	5.50	CI	0.56	AZ	5.50	12.12
CJ	CJ	0.30	BI	1.45	CH	0.72	AQ	10.60	13.07

Design Tandem - Single Loaded Lane
Superposition Method
Total Wheel Loading
This spreadsheet calculates the total stress at each point based on all four wheel loads (1-4)
Note: All stresses are in psf
Note: All depths and load conditions are calculated in a similar manner

Table A-5. Superposition stress calculation summary, tandem 1 lane

z = 2

Point	r	Stress
U	10	2
T	8	6
CJ	7	13
S	6	31
CE	5	84
R	4	266
BJ	3.5	475
BI	3	792
BH	2.5	1135
Q	2	1300
BG	1.5	1165
BF	1	861
BE	0.5	611
P	0	521
BD	-0.5	611
BC	-1	861
BB	-1.5	1165
O	-2	1300
BH	-2.5	1135
BI	-3	792
BJ	-3.5	475
R	-4	266
CE	-5	84
S	-6	31
CJ	-7	13
T	-8	6
U	-10	2

z = 3

Point	r	Stress
U	10	6
T	8	17
CJ	7	30
S	6	62
CE	5	132
R	4	281
BJ	3.5	394
BI	3	520
BH	2.5	629
Q	2	684
BG	1.5	673
BF	1	616
BE	0.5	557
P	0	533
BD	-0.5	557
BC	-1	616
BB	-1.5	673
O	-2	684
BH	-2.5	629
BI	-3	520
BJ	-3.5	394
R	-4	281
CE	-5	132
S	-6	62
CJ	-7	30
T	-8	17
U	-10	6

z = 4

Point	r	Stress
U	10	11
T	8	29
CJ	7	47
S	6	85
CE	5	149
R	4	250
BJ	3.5	311
BI	3	371
BH	2.5	421
Q	2	453
BG	1.5	466
BF	1	462
BE	0.5	454
P	0	450
BD	-0.5	454
BC	-1	462
BB	-1.5	466
O	-2	453
BH	-2.5	421
BI	-3	371
BJ	-3.5	311
R	-4	250
CE	-5	149
S	-6	85
CJ	-7	47
T	-8	29
U	-10	11

z = 5

Point	r	Stress
U	10	18
T	8	40
CJ	7	60
S	6	98
CE	5	150
R	4	218
BJ	3.5	255
BI	3	290
BH	2.5	320
Q	2	342
BG	1.5	357
BF	1	364
BE	0.5	367
P	0	368
BD	-0.5	367
BC	-1	364
BB	-1.5	357
O	-2	342
BH	-2.5	320
BI	-3	290
BJ	-3.5	255
R	-4	218
CE	-5	150
S	-6	98
CJ	-7	60
T	-8	40
U	-10	18

z = 6

Point	r	Stress
N	10	26
M	8	54
CI	7	78
L	6	110
CD	5	151
K	4	197
BA	3.5	221
AZ	3	243
AY	2.5	263
J	2	279
AX	1.5	292
AW	1	301
AV	0.5	306
I	0	307
AU	-0.5	306
AT	-1	301
AS	-1.5	292
H	-2	279
AY	-2.5	263
AZ	-3	243
BA	-3.5	221
K	-4	197
CD	-5	151
L	-6	110
CI	-7	78
M	-8	54
N	-10	26

z = 8

Point	r	Stress
N	10	37
M	8	65
CI	7	85
L	6	109
CD	5	137
K	4	166
BA	3.5	181
AZ	3	194
AY	2.5	206
J	2	215
AX	1.5	224
AW	1	230
AV	0.5	233
I	0	234
AU	-0.5	233
AT	-1	230
AS	-1.5	224
H	-2	215
AY	-2.5	206
AZ	-3	194
BA	-3.5	181
K	-4	166
CD	-5	137
L	-6	109
CI	-7	85
M	-8	65
N	-10	37

z = 10

Point	r	Stress
N	10	42
M	8	66
CI	7	81
L	6	98
CD	5	117
K	4	135
BA	3.5	143
AZ	3	151
AY	2.5	158
J	2	164
AX	1.5	169
AW	1	173
AV	0.5	175
I	0	175
AU	-0.5	175
AT	-1	173
AS	-1.5	169
H	-2	164
AY	-2.5	158
AZ	-3	151
BA	-3.5	143
K	-4	135
CD	-5	117
L	-6	98
CI	-7	81
M	-8	66
N	-10	42

z = 12

Point	r	Stress
N	10	43
M	8	62
CI	7	73
L	6	85
CD	5	97
K	4	109
BA	3.5	114
AZ	3	119
AY	2.5	123
J	2	126
AX	1.5	129
AW	1	132
AV	0.5	133
I	0	133
AU	-0.5	133
AT	-1	132
AS	-1.5	129
H	-2	126
AY	-2.5	123
AZ	-3	119
BA	-3.5	114
K	-4	109
CD	-5	97
L	-6	85
CI	-7	73
M	-8	62
N	-10	43

r = distance to centerline of axle spacing (ft)
Critical line is one between the two wheels at depts greater than 5 ft
Stress in psf

Table A-6. Buried pipe calculations

Culvert	H (ft)	p (psf)	D (ft)	M (ft)	D/2H	M/2H	Cs	F'	Bc (ft)	Wsd (lb/ft)	σ_z (psf)
H = 2'											
12' x 12'	2	9000	1.666	0.833	0.4165	0.20825	0.1399	1.25	12	18886.5	1573.88
10' x 10'	2	9000	1.666	0.833	0.4165	0.20825	0.1399	1.25	10	15738.75	1573.88
8' x 8'	2	9000	1.666	0.833	0.4165	0.20825	0.1399	1.25	8	12591	1573.88
6' x 6'	2	9000	1.666	0.833	0.4165	0.20825	0.1399	1.25	6	9443.25	1573.88
H = 3'											
12' x 12'	3	9000	1.666	0.833	0.27767	0.13883	0.0649	1.15	12	8060.58	671.715
10' x 10'	3	9000	1.666	0.833	0.27767	0.13883	0.0649	1.15	10	6717.15	671.715
8' x 8'	3	9000	1.666	0.833	0.27767	0.13883	0.0649	1.15	8	5373.72	671.715
6' x 6'	3	9000	1.666	0.833	0.27767	0.13883	0.0649	1.15	6	4030.29	671.715
H = 4'											
12' x 12'	4	9000	1.666	0.833	0.20825	0.10413	0.03774	1	12	4075.92	339.66
10' x 10'	4	9000	1.666	0.833	0.20825	0.10413	0.03774	1	10	3396.6	339.66
8' x 8'	4	9000	1.666	0.833	0.20825	0.10413	0.03774	1	8	2717.28	339.66
6' x 6'	4	9000	1.666	0.833	0.20825	0.10413	0.03774	1	6	2037.96	339.66
H = 5'											
12' x 12'	5	9000	1.666	0.833	0.1666	0.0833	0.02965	1	12	3202.2	266.85
10' x 10'	5	9000	1.666	0.833	0.1666	0.0833	0.02965	1	10	2668.5	266.85
8' x 8'	5	9000	1.666	0.833	0.1666	0.0833	0.02965	1	8	2134.8	266.85
6' x 6'	5	9000	1.666	0.833	0.1666	0.0833	0.02965	1	6	1601.1	266.85
H = 6'											
12' x 12'	6	9000	1.666	0.833	0.13883	0.06942	0.0252	1	12	2721.6	226.8
10' x 10'	6	9000	1.666	0.833	0.13883	0.06942	0.0252	1	10	2268	226.8
8' x 8'	6	9000	1.666	0.833	0.13883	0.06942	0.0252	1	8	1814.4	226.8
6' x 6'	6	9000	1.666	0.833	0.13883	0.06942	0.0252	1	6	1360.8	226.8
H = 8'											
12' x 12'	8	9000	1.666	0.833	0.10413	0.05206	0.01965	1	12	2122.2	176.85
10' x 10'	8	9000	1.666	0.833	0.10413	0.05206	0.01965	1	10	1768.5	176.85
8' x 8'	8	9000	1.666	0.833	0.10413	0.05206	0.01965	1	8	1414.8	176.85
6' x 6'	8	9000	1.666	0.833	0.10413	0.05206	0.01965	1	6	1061.1	176.85
H = 10'											
12' x 12'	10	9000	1.666	0.833	0.0833	0.04165	0.019	1	12	2052	171
10' x 10'	10	9000	1.666	0.833	0.0833	0.04165	0.019	1	10	1710	171
8' x 8'	10	9000	1.666	0.833	0.0833	0.04165	0.019	1	8	1368	171
6' x 6'	10	9000	1.666	0.833	0.0833	0.04165	0.019	1	6	1026	171
H = 12'											
12' x 12'	12	9000	1.666	0.833	0.06942	0.03471	0.019	1	12	2052	171
10' x 10'	12	9000	1.666	0.833	0.06942	0.03471	0.019	1	10	1710	171
8' x 8'	12	9000	1.666	0.833	0.06942	0.03471	0.019	1	8	1368	171
6' x 6'	12	9000	1.666	0.833	0.06942	0.03471	0.019	1	6	1026	171

Newmark's integration of the Boussinesq point load solution
Load is centered vertically over the culvert
Wsd = CspF'Bc   Wsd = load on pipe (lbs/length)
Cs = load coefficient based on D/2H and M/2H (from table)
D = width of area that distributed load acts
M = Length of area that distributed load acts
H = Depth of fill
F' = Impact Factor from table in text
p = distributed load
Bc = diameter of pipe

Sample calculation of culvert stresses using the AASHTO method

Design Tandem

NOTE : Calculations are similar for all depths and load conditions

Wheel Load 1: $P1 := 12.5$ (P is in kips, distances are in feet)

Wheel Load 2: $P2 := 12.5$

Wheel Load 3: $P3 := 0$ Zero because the front axle load is insignificant

Axle Spacing 1: $spa1 := 4$ Distance between rear tandem axles

Axle Spacing 2: $spa2 := 0$ Zero becasue the front axle is insignificant

Wheel Spacing: $ws := 6$

$TireWidth := 1.666$

$TireLength := .832$

Depth of Fill: $H := 12$

Soil Distribution Factor: $SDF := 1.15$

Impact Factor: $IM := 33\cdot(1 - .125\cdot H)\cdot.01$ $IM = -0.165$

$Tt := .666$

$$stress(P, L, W) := \frac{P}{L\cdot W}$$

twL1 : Length of the loaded area at the depth in question for the 1st wheel load

tw1 : Stress from the first wheel load at the depth in question

NOTE :
The stress from each distributed load is simply calculated as Stress = P/(L*W), where P is the axle load, L is the effective load length calculated previously, and W is the width of the load. The calculation is therefore based on the geometry of the loading condition. Although in some cases the effective length of a wheel load is zero, it is compensated for by including its force in another place. For example, if both twL2 and twL3 are zero because twL1 encompasses the whole area, all three loads (P1, P2 and P3) are used to calculate the stress from first distributed load. If twL2 is zero and twL3 is defined, then P1 and P2 are only used to calculate the first distributed load because twL1 doesn't include any area loaded by P3. The initial width (20 inches) is also increased by H*SDF, but in some loading cases it is also increased by ws.

The process to find the stress is broken into three test conditions: H*SDF>ws-tire width; H*SDF > 4 feet - tire width; H > 2 feet. These three main conditions are then broken in to two "tests" each. Test1 is the one loaded lane situation, and Test2 is the two lane situation. Test2 uses double the loads (4*P1 as oppose to 2*P1) that Test1 does. The stress is found for each test, and then it is multiplied by the multiple presence factor. For 1 lane, m=1.2 and for 2 lanes, m=1.0. The larger of the two tests is taken as the stress for that loading condition.

Figure A-1. Sample AASHTO stress calculations

$$
\mathrm{twL1}(P1,P2,P3,spa1,spa2,H) := \left|\begin{array}{l}
\text{if } H\cdot SDF \ge spa1 - TireLength\cdot .5 + TireLength\cdot .5 \\
\quad \left|\begin{array}{l}
\text{if } [\,[\,H\cdot SDF \ge spa2 - (TireLength\cdot .5 + TireLength\cdot .5)\,]\,] \\
\quad \left|\begin{array}{l}
\left(spa1 + spa2 + \dfrac{TireLength}{2} + \dfrac{TireLength}{2} + H\cdot SDF\right) \ \text{if } P3 \ne 0 \\
\text{otherwise} \\
\quad \left|\begin{array}{l}
\left(spa1 + \dfrac{TireLength}{2} + \dfrac{TireLength}{2} + H\cdot SDF\right) \ \text{if } P2 \ne 0 \\
(TireLength + H\cdot SDF) \ \text{otherwise}
\end{array}\right.
\end{array}\right. \\
\left(spa1 + \dfrac{TireLength}{2} + \dfrac{TireLength}{2} + H\cdot SDF\right) \ \text{otherwise}
\end{array}\right. \\
\text{otherwise} \\
\quad \left|\begin{array}{l}
(TireLength + Tt) \ \text{if } H \le 2 \\
(TireLength + H\cdot SDF) \ \text{otherwise}
\end{array}\right.
\end{array}\right.
$$

$$\mathrm{twL1}(P1,P2,P3,spa1,spa2,H) = \blacksquare$$

$$
\mathrm{twL3}(P1,P2,P3,spa1,spa2,H) := \left|\begin{array}{l}
0 \ \text{if } H\cdot SDF \ge spa2 - (TireLength\cdot .5 + TireLength\cdot .5) \\
\text{otherwise} \\
\quad \left|\begin{array}{l}
(TireLength + Tt) \ \text{if } H \le 2 \\
(TireLength + H\cdot SDF) \ \text{otherwise}
\end{array}\right.
\end{array}\right.
$$

$$\mathrm{twL3}(P1,P2,P3,spa1,spa2,H) = \blacksquare$$

$$
\mathrm{twL2}(P1,P2,P3,spa1,spa2,H) := \left|\begin{array}{l}
0 \ \text{if } H\cdot SDF \ge spa1 - (TireLength\cdot .5 + TireLength\cdot .5) \\
\text{otherwise} \\
\quad \left|\begin{array}{l}
\text{if } H\cdot SDF \ge spa2 \\
\quad \left|\begin{array}{l}
(TireLength + Tt) \ \text{if } H \le 2 \\
\text{otherwise} \\
\quad \left|\begin{array}{l}
(TireLength + H\cdot SDF) \ \text{if } P3 \le 0 \\
[(TireLength + TireLength)\cdot .5 + spa2 + H\cdot SDF] \ \text{otherwise}
\end{array}\right.
\end{array}\right. \\
\text{otherwise} \\
\quad \left|\begin{array}{l}
(TireLength + Tt) \ \text{if } H \le 2 \\
(TireLength + H\cdot SDF) \ \text{otherwise}
\end{array}\right.
\end{array}\right.
\end{array}\right.
$$

$$\mathrm{twL2}(P1,P2,P3,spa1,spa2,H) = \blacksquare$$

Figure A-1. Continued

```
tw1(P1, P2, P3, twL1, twL2, twL3, H, ws) := | if H·SDF > ws − TireWidth
                                            |   if twL2 = 0
                                            |     if twL3 = 0
                                            |       test2 ← stress[4·(P1 + P2 + P3), twL1, 2·ws + 4 + TireWidth + H·SDF]·1
                                            |       test1 ← stress[2·(P1 + P2 + P3), twL1, ws + TireWidth + H·SDF]·1.2
                                            |     otherwise
                                            |       test2 ← stress[4·(P1 + P2), twL1, 2·ws + 4 + TireWidth + H·SDF]·1
                                            |       test1 ← stress[2·(P1 + P2), twL1, ws + TireWidth + H·SDF]·1.2
                                            |   otherwise
                                            |     test2 ← stress(4·P1, twL1, 2·ws + 4 + TireWidth + H·SDF)·1
                                            |     test1 ← stress(2·P1, twL1, ws + TireWidth + H·SDF)·1.2
                                            | otherwise
                                            |   if H·SDF > 4 − TireWidth
                                            |     if twL2 = 0
                                            |       if twL3 = 0
                                            |         test2 ← stress[2·(P1 + P2 + P3), twL1, 4 + TireWidth + H·SDF]·1
                                            |         test1 ← stress(P1 + P2 + P3, twL1, TireWidth + H·SDF)·1.2
                                            |       otherwise
                                            |         test2 ← [2·(P1 + P2), twL1, 4 + TireWidth + H·SDF]·1
                                            |         test1 ← (P1 + P2, twL1, TireWidth + H·SDF)·1.2
                                            |     otherwise
                                            |       test2 ← stress(2·P1, twL1, 4 + TireWidth + H·SDF)·1
                                            |       test1 ← stress(P1, twL1, TireWidth + H·SDF)·1.2
                                            |   otherwise
                                            |     if H > 2
                                            |       test2 ← 0
                                            |       test1 ← stress(P1, twL1, TireWidth + H·SDF)·1.2
                                            |     otherwise
                                            |       test2 ← stress(P1, twL1, TireWidth) 1
                                            |       test1 ← stress(P1, twL1, TireWidth)·1.2
                                            | test ← test1
                                            | test ← test2  if test2 > test1
                                            | test
```

tw1(P1, P2, P3, 18.632, 0, 0, H, ws) = ▮

Figure A-1. Continued

```
tw2(P2, P3, twL2, twL3, H, ws) := | 0  if twL2 = 0
                                  | otherwise
                                  |   if H·SDF > (ws − TireWidth)
                                  |     if twL3 = 0
                                  |       test2 ← stress [4·(P2 + P3), twL2, 2·ws + 4 + TireWidth + H·SDF]·1
                                  |       test1 ← stress [2·(P2 + P3), twL2, TireWidth + ws + H·SDF]·1.2
                                  |     otherwise
                                  |       test2 ← stress [4·(P2), twL2, 2·ws + 4 + TireWidth + H·SDF]·1
                                  |       test1 ← stress (2·P2, twL2, TireWidth + ws + H·SDF) 1.2
                                  |   otherwise
                                  |     if H·SDF > 4 − TireWidth
                                  |       if twL3 = 0
                                  |         test2 ← stress [2·(P2 + P3), twL2, 4 + TireWidth + H·SDF]·1
                                  |         test1 ← stress (P2 + P3, twL2, TireWidth + H·SDF)·1.2
                                  |       otherwise
                                  |         test2 ← stress [2·(P2), twL2, 4 + TireWidth + H·SDF]·1
                                  |         test1 ← stress (P2, twL2, TireWidth + H·SDF)·1.2
                                  |     otherwise
                                  |       if H > 2
                                  |         test2 ← 0
                                  |         test1 ← stress (P2, twL2, TireWidth + H·SDF)·1.2
                                  |       otherwise
                                  |         test2 ← stress (P2, twL2, TireWidth)·1
                                  |         test1 ← stress (P2, twL2, TireWidth)·1.2
                                  |   test ← test1
                                  |   test ← test2  if test2 > test1
                                  |   test

tw2(P2, P3, 3.132, 0, H, ws) = ▮
```

Figure A-1. Continued

```
tw3(P3, twL3, H, ws) := | 0  if twL3 = 0
                        | otherwise
                        |   | if H·SDF > (ws − TireWidth)
                        |   |   | test2 ← stress[4·(P3), twL3, 2·ws + 4 + TireWidth + H·SDF]·1
                        |   |   | test1 ← stress(2·P3, twL3, TireWidth + ws + H·SDF)·1.2
                        |   | otherwise
                        |   |   | if H·SDF > 4 − TireWidth
                        |   |   |   | test2 ← stress[2·(P3), twL3, 4 + TireWidth + H·SDF]·1
                        |   |   |   | test1 ← stress(P3, twL3, TireWidth + H·SDF)·1.2
                        |   |   | otherwise
                        |   |   |   | if H > 2
                        |   |   |   |   | test2 ← 0
                        |   |   |   |   | test1 ← stress(P3, twL3, TireWidth + H·SDF)·1.2
                        |   |   |   | otherwise
                        |   |   |   |   | test2 ← stress(P3, twL3, TireWidth)·1
                        |   |   |   |   | test1 ← stress(P3, twL3, TireWidth)·1.2
                        |   | test ← test1
                        |   | test ← test2  if test2 > test1
                        |   | test
```

tw3(P3, 0, H, ws) = ▮

Figure A-1. Continued

APPENDIX B
EQUIVALENT UNIFORM LOAD CALCULATIONS

TANDEM - 1 LOADED LANE
z = 2'
SPAN = 6'

Load

NumPoints := 13

ii := ORIGIN.. NumPoints − 1

$$\text{load} := \begin{pmatrix} 791.76 \\ 1135.47 \\ 1300.39 \\ 1164.65 \\ 860.94 \\ 611.19 \\ 521.33 \\ 611.19 \\ 860.94 \\ 1164.65 \\ 1300.39 \\ 1135.47 \\ 791.76 \end{pmatrix}$$

x-values: Distance from center of wheel spacing

SpanLength := 6

$$x := \begin{pmatrix} -3 \\ -2.5 \\ -2 \\ -1.5 \\ -1 \\ -0.5 \\ 0 \\ 0.5 \\ 1 \\ 1.5 \\ 2 \\ 2.5 \\ 3 \end{pmatrix}$$

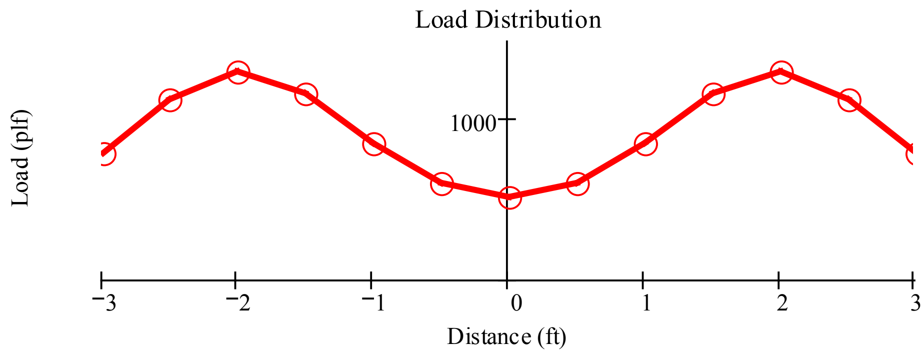

Solve for Reactions

Figure B-1 Sample equivalent uniform load calculation

Solve for Reactions

$$\text{AreaTotal} := \left| \begin{array}{l} \text{sum} \leftarrow 0 \\ \text{for } i \in \text{ORIGIN}..\text{last}(x) - 1 \\ \quad \text{sum} \leftarrow \text{sum} + \left(\frac{\left| \text{load}_i + \text{load}_{i+1} \right|}{2} \right) \cdot \left| x_i - x_{i+1} \right| \\ \text{return sum} \end{array} \right.$$

$\text{AreaTotal} = 5729.19$

$i := \text{ORIGIN}..\text{NumPoints} - 2$

$$\text{area}(i) := \left(\frac{\left| \text{load}_i + \text{load}_{i+1} \right|}{2} \right) \cdot \left| x_i - x_{i+1} \right|$$

$$d(i) := \begin{cases} \left[\left[x_{i+1} + \left[(-x)_{\text{ORIGIN}} \right] \right] - \left[\left[\frac{\left| x_{i+1} - x_i \right|}{3} \cdot \frac{\left(2 \cdot \text{load}_i + \text{load}_{i+1} \right)}{\text{load}_i + \text{load}_{i+1}} \right] \right] \right] & \text{if } \text{load}_{i+1} \geq \text{load}_i \\ \left[\left[x_i + \left[(-x)_{\text{ORIGIN}} \right] \right] + \left[\frac{\left| x_{i+1} - x_i \right|}{3} \cdot \frac{\left(2 \cdot \text{load}_{i+1} + \text{load}_i \right)}{\text{load}_i + \text{load}_{i+1}} \right] \right] & \text{otherwise} \end{cases}$$

$$R_b := \frac{\left[\sum_i (\text{area}(i) \cdot d(i)) \right]}{\text{SpanLength}} \qquad R_a := \text{AreaTotal} - R_b \qquad R_b = 2864.59 \qquad R_a = 2864.59$$

Calculate Shears

$$V := \left| \begin{array}{l} V_{\text{ORIGIN}} \leftarrow R_a \\ \text{for } ii \in \text{ORIGIN} + 1..\text{last}(x) \\ \quad V_{ii} \leftarrow V_{ii-1} - \frac{1}{2} \cdot \left(\text{load}_{ii} + \text{load}_{ii-1} \right) \cdot \left(x_{ii} - x_{ii-1} \right) \\ V \end{array} \right.$$

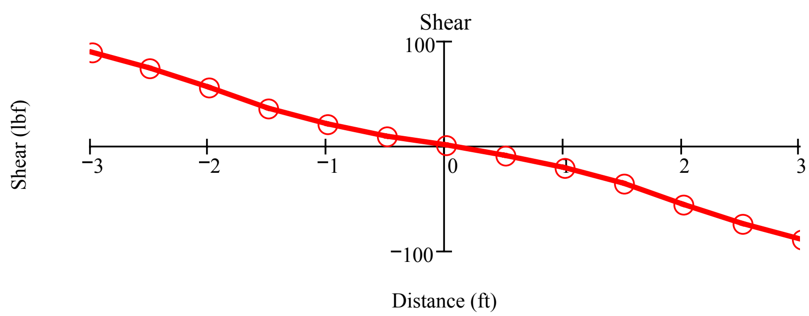

$V_{\text{last}(V)} = -2864.59$ check: should equal $-R_b = -2864.59$

Figure B-1. Continued

Calculate Moments (assuming simple supports)

$$M := \left| \begin{array}{l} M_{ORIGIN} \leftarrow 0 \\ \text{for } ii \in ORIGIN + 1 .. last(x) \\ \quad M_{ii} \leftarrow M_{ii-1} + \frac{1}{2} \cdot \left(V_{ii} + V_{ii-1}\right) \cdot \left(x_{ii} - x_{ii-1}\right) \\ M \end{array} \right.$$

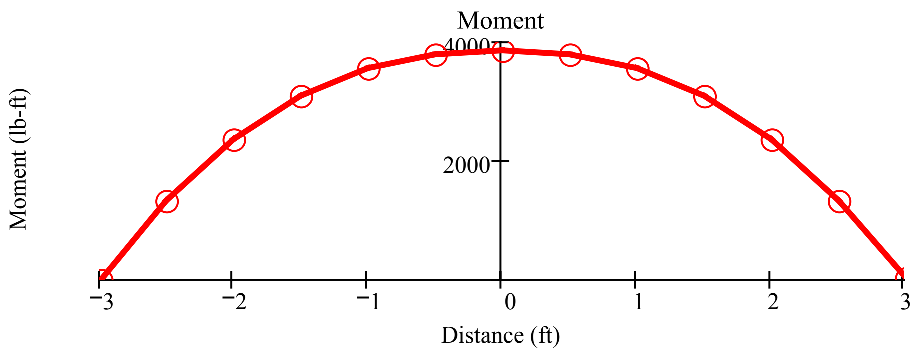

$M_{last(M)} = 0$ check: should equal 0

$max(V) = 2864.59$ $max(M) = 3840.38$

$q_M := \frac{8}{SpanLength^2} \cdot max(M)$ $q_M = 853.42$ $q_V := \frac{2}{SpanLength} \cdot max(V)$ $q_V = 954.86$

$$q := \left| \begin{array}{l} q_M \text{ if } q_M \geq q_V \\ q_V \text{ otherwise} \end{array} \right.$$

$q = 954.86$

Figure B-1. Continued

Table B-1. Equivalent uniform load summary, tandem 1 lane

z = 2'

Culvert span (ft)	Max shear (lb)	Max moment (lb-ft)	Equivalent load (lb/ft)
6	2865	3840	955
8	3366.8	6988.9	873.61
10	3542.12	10443.4	835.47
12	3599.5	14014.2	778.5
14	3621.4	17624.67	719.37

z = 3'

Culvert span (ft)	Max shear (lb)	Max moment (lb-ft)	Equivalent load (lb/ft)
6	1842.67	2715.21	614
8	2240.17	4771.6	596.45
10	2446.68	7115	569.2
12	2543.66	9610.17	533.9
14	2589.84	12176.92	497.02

z = 4'

Culvert span (ft)	Max shear (lb)	Max moment (lb-ft)	Equivalent load (lb/ft)
6	1333.74	2044.02	454.23
8	1644.57	3540.76	442.6
10	1844.1	5285.1	422.81
12	1961.23	7187.77	399.32
14	2027.46	9182.11	374.78

z = 5'

Culvert span (ft)	Max shear (lb)	Max moment (lb-ft)	Equivalent load (lb/ft)
6	1039.32	1613.08	358.46
8	1293.47	2783.97	348
10	1477.16	4169.28	333.54
12	1600.82	5708.27	317.13
14	1679.57	7348.47	299.94

z = 6'

Culvert span (ft)	Max shear (lb)	Max moment (lb-ft)	Equivalent load (lb/ft)
6	858.12	1334.23	296.49
8	1078.88	2305.59	288.2
10	1253.04	3471.55	277.72
12	1383.34	4789.74	266.1
14	1477.01	6219.91	253.87

z = 8'

Culvert span (ft)	Max shear (lb)	Max moment (lb-ft)	Equivalent load (lb/ft)
6	661.07	1021.74	227.05
8	841.45	1774.72	221.84
10	993.37	2692.13	215.37
12	1116.84	3747.24	208.18
14	1214.11	4912.71	200.52

z = 10'

Culvert span (ft)	Max shear (lb)	Max moment (lb-ft)	Equivalent load (lb/ft)
6	501.02	769.48	171
8	644.2	1343.12	167.89
10	769.95	2050.19	164.02
12	877.57	2873.95	159.66
14	967.47	3796.47	154.96

z = 12'

Culvert span (ft)	Max shear (lb)	Max moment (lb-ft)	Equivalent load (lb/ft)
6	384.65	587.76	130.61
8	498.4	1029.93	128.74
10	601.24	1579.75	126.38
12	692.38	2226.56	123.7
14	771.62	2958.56	120.76

Table B-2. Equivalent uniform load summary, tandem 2 lanes

z = 2'

Culvert span (ft)	Max shear (lb)	Max moment (lb-ft)	Equivalent load (lb/ft)
6	2990.49	4032	997
8	3521.2	7321.49	915.19
10	3713.44	10938.81	875.1
12	3779.78	14685.42	815.86
14	3806.06	18478.34	754.22

z = 3'

Culvert span (ft)	Max shear (lb)	Max moment (lb-ft)	Equivalent load (lb/ft)
6	2059.11	3049.14	686
8	2506.94	5348.29	668.54
10	2746.03	7974.78	637.98
12	2861.88	10778.74	598.82
14	2918.65	13669	557.92

z = 4'

Culvert span (ft)	Max shear (lb)	Max moment (lb-ft)	Equivalent load (lb/ft)
6	1684.72	2596.41	576.98
8	2080.53	4488	561
10	2341.68	6699.11	535.93
12	2498.66	9119.28	506.63
14	2589.31	11663.26	476.05

z = 5'

Culvert span (ft)	Max shear (lb)	Max moment (lb-ft)	Equivalent load (lb/ft)
6	1400.23	2176.77	483.73
8	1742.48	3754.06	469.26
10	1990.93	5620.77	449.66
12	2158.34	7695.4	427.52
14	2266.18	9907.65	404.39

z = 6'

Culvert span (ft)	Max shear (lb)	Max moment (lb-ft)	Equivalent load (lb/ft)
6	1153.69	1795.18	398.93
8	1446.11	3099.18	387.4
10	1672.1	4658.28	372.66
12	1836.82	6412.74	356.26
14	1951.91	8307.1	339.07

z = 8'

Culvert span (ft)	Max shear (lb)	Max moment (lb-ft)	Equivalent load (lb/ft)
6	794.48	1229.36	273.19
8	1009.23	2133.36	266.67
10	1188.46	3232.21	258.58
12	1332.45	4492.66	249.59
14	1444.42	5881.1	240.04

z = 10'

Culvert span (ft)	Max shear (lb)	Max moment (lb-ft)	Equivalent load (lb/ft)
6	567.36	872.08	193.8
8	728.58	1521.26	190.16
10	869.49	2320.29	185.62
12	989.36	3249.72	180.54
14	1088.82	4288.81	175.05

z = 12'

Culvert span (ft)	Max shear (lb)	Max moment (lb-ft)	Equivalent load (lb/ft)
6	420.59	643.02	142.89
8	544.55	1126.31	140.79
10	656.29	1726.73	138.14
12	754.98	2432.36	135.13
14	840.44	3230.07	131.84

Table B-3. Equivalent uniform load summary, truck 1 lane

z = 2'

Culvert span (ft)	Max shear (lb)	Max moment (lb-ft)	Equivalent load (lb/ft)
6	2205.81	4573.45	1016.32
8	2272.13	6819.59	852.07
10	2299.4	9102.35	728.19
12	2312.5	11408.3	633.79
14	2321	13725.1	560.21

z = 3'

Culvert span (ft)	Max shear (lb)	Max moment (lb-ft)	Equivalent load (lb/ft)
6	1462.44	2726.28	605.84
8	1575.94	4250.74	531.34
10	1633.56	5856.49	468.44
12	1665.87	7505.2	416.96
14	1688.87	9182.57	374.8

z = 4'

Culvert span (ft)	Max shear (lb)	Max moment (lb-ft)	Equivalent load (lb/ft)
6	1048.29	1821.93	404.87
8	1184.42	2942.86	367.86
10	1266.74	4168.44	333.48
12	1319.96	5461.79	303.43
14	1361.07	6802.31	277.65

z = 5'

Culvert span (ft)	Max shear (lb)	Max moment (lb-ft)	Equivalent load (lb/ft)
6	800.87	1330.25	295.61
8	942.01	2205.09	275.64
10	1039.64	3195.92	255.67
12	1110.48	4270.98	237.28
14	1169.09	5410.76	220.85

z = 6'

Culvert span (ft)	Max shear (lb)	Max moment (lb-ft)	Equivalent load (lb/ft)
6	642.62	1035.82	230.18
8	780.11	1749.57	218.7
10	885.23	2582.24	206.58
12	968.57	3509.14	194.95
14	1041.29	4514.06	184.25

z = 8'

Culvert span (ft)	Max shear (lb)	Max moment (lb-ft)	Equivalent load (lb/ft)
6	497.66	772.98	171.77
8	631.45	1338.72	167.34
10	748.05	2028.47	162.28
12	851.77	2828.38	157.13
14	978.67	3728.6	152.19

z = 10'

Culvert span (ft)	Max shear (lb)	Max moment (lb-ft)	Equivalent load (lb/ft)
6	385.98	588.44	130.76
8	501.67	1032.79	129.1
10	609.42	1588.34	127.07
12	710.96	2248.53	124.92
14	809.12	3008.57	122.8

z = 12'

Culvert span (ft)	Max shear (lb)	Max moment (lb-ft)	Equivalent load (lb/ft)
6	308.09	464.09	103.13
8	406.64	821.66	102.71
10	501.98	1275.96	102.08
12	594.73	1824.31	101.35
14	686.02	2464.69	100.6

Table B-4. Equivalent uniform load summary, truck 2 lanes

z = 2'

Culvert span (ft)	Max shear (lb)	Max moment (lb-ft)	Equivalent load (lb/ft)
6	2305.7	4751.09	1055.8
8	2382.6	7099.85	887.48
10	2415.38	9498.84	759.91
12	2431.46	11922.26	662.35
14	24442.03	14359	560.21

z = 3'

Culvert span (ft)	Max shear (lb)	Max moment (lb-ft)	Equivalent load (lb/ft)
6	1632.53	3019.91	671.09
8	1768.29	4726.4	590.8
10	1838.62	6529.86	522.39
12	1878.4	8388.37	466.02
14	1906.68	10280.91	419.63

z = 4'

Culvert span (ft)	Max shear (lb)	Max moment (lb-ft)	Equivalent load (lb/ft)
6	1319.6	2267.76	503.95
8	1502.41	3684.7	460.59
10	1613.82	5242.82	419.43
12	1685.35	5461.79	382.91
14	1361.07	8605.05	351.23

z = 5'

Culvert span (ft)	Max shear (lb)	Max moment (lb-ft)	Equivalent load (lb/ft)
6	1076.52	1783.14	396.25
8	1268.06	2960.09	370.01
10	1399.51	4293.88	343.51
12	1493.5	5740.38	318.91
14	1570.25	7272.25	296.83

z = 6'

Culvert span (ft)	Max shear (lb)	Max moment (lb-ft)	Equivalent load (lb/ft)
6	873.77	1409	313.32
8	1058.49	2379.44	297.43
10	1197.77	3507.57	280.61
12	1306.36	4759.63	264.42
14	1041.29	6112.8	249.5

z = 8'

Culvert span (ft)	Max shear (lb)	Max moment (lb-ft)	Equivalent load (lb/ft)
6	597.05	931.21	206.94
8	753.59	1608.07	201.01
10	887.9	2428.81	194.3
12	1005.72	3375.62	187.53
14	1114.88	4435.92	181.06

z = 10'

Culvert span (ft)	Max shear (lb)	Max moment (lb-ft)	Equivalent load (lb/ft)
6	435.15	664.82	147.74
8	564.03	1165.07	145.63
10	609.42	1788.68	143.09
12	794.8	2527.67	140.43
14	902.3	3376.22	137.8

z = 12'

Culvert span (ft)	Max shear (lb)	Max moment (lb-ft)	Equivalent load (lb/ft)
6	335.18	464.09	112.33
8	441.77	894.2	111.78
10	544.53	1387.35	110.99
12	644.23	1981.73	110.1
14	742.21	2674.95	109.18

Table B-5. Best fit equation summary

Depth (ft)	Uniform distributed load (q), plf											
	Tandem 1 lane			Tandem 2 lane			Truck 1 lane			Truck 2 lane		
	Eq 4.1	Eq 4.5	Calc	Eq 4.2	Eq 4.6	Calc	Eq 4.3	Eq 4.7	Calc	Eq 4.4	Eq 4.8	Calc
2	906	954	955	870	1014	997	991	1017	1016	1161	1066	1056
3	591	619	614	698	700	686	591	597	606	692	671	671
4	437	455	454	575	538	577	410	409	405	480	483	504
5	345	358	358	480	439	484	308	305	296	361	374	396
6	285	295	296	403	372	399	244	240	230	286	304	313
7	242	250	---	337	323	---	201	196	---	235	255	---
8	211	217	227	280	286	273	169	165	172	198	219	207
9	186	191	---	230	257	---	146	141	---	171	191	---
10	167	171	171	185	233	194	127	123	131	149	169	148
11	151	154	---	145	214	---	113	108	---	132	152	---
12	137	141	131	108	198	143	101	97	103	118	138	103

NOTE: --- indicates where data was not calculated

REFERENCES

1. Rund, R.E. and McGrath, T.J., "Comparison of AASHTO Standard and LRFD Code Provisions for Buried Concrete Box Culverts," *Concrete Pipe for the New Millennium*, ASTM STP 1368, I.I Kaspar and J.I. Enyart, Eds., American Society for Testing and Materials, West Conshohocken, Pennsylvania, 2000, pp. 45-60.

2. American Association of State Highway and Transportation Officials (AASHTO), *LRFD Bridge Design Specifications*, Second Edition, American Association of State Highway and Transportation Officials, Washington, D.C., 1998.

3. AASHTO, *Standard Specification for Highway Bridges*, 16th Edition, American Association of State Highway and Transportation Officials, Washington, D.C., 1996.

4. Holtz, R. D. and Kovacs, W. D. *An Introduction to Geotechnical Engineering*. Englewood Cliffs, New Jersey: Prentice-Hall, 1981.

5. Moser, A.P. *Buried Pipe Design*. New York: McGraw-Hill, 2001.

6. ASCE, *Standard Practice for Direct Design of Buried Precast Concrete Pipe Using Standard Installations (SIDD)*, (ASCE 15-98), American Society of Civil Engineers, Reston, Virginia, 2000.

7. James, R. W. and Brown, D. E., "Wheel-Load-Induced Earth Pressures on Box Culverts," *Transportation Research Record 1129*, TRB, National Research Counsel, Washington, D.C., 1987, pp. 55-62.

8. Abdel-Karim, A.M., Tadros, M.K., and Benak, J.V., "Live Load Distribution on Concrete Box Culverts," *Transportation Research Record 1288*, TRB, National Research Counsel, Washington, D.C., 1990, pp. 136-151.